Full length article

Agonistic and potentiating effects of perfluoroalkyl substances (PFAS) on the Atlantic cod (*Gadus morhua*) peroxisome proliferator-activated receptors (Ppars)

Sofie Søderstrøm [a,c], Roger Lille-Langøy [a,c], Fekadu Yadetie [a], Mateusz Rauch [b], Ana Milinski [b], Annick Dejaegere [b], Roland H. Stote [b], Anders Goksøyr [a], Odd André Karlsen [a,*]

[a] *Department of Biological Sciences, University of Bergen, Thormøhlens gate 53 A/B, NO-5006 Bergen, Norway*
[b] *Department of Integrated Structural Biology, Institut de Génétique et de Biologie Moléculaire et Cellulaire (IGBMC), Institut National de La Santé et de La Recherche Médicale (INSERM), U1258/Centre National de Recherche Scientifique (CNRS), UMR7104/Université de Strasbourg, Illkirch, France*
[c] *Institute of Marine Research, Nordnesgaten 50, NO-5005 Bergen, Norway[1]*

ARTICLE INFO

ABSTRACT

Toxicity mediated by per- and polyfluoroalkyl substances (PFAS), and especially perfluoroalkyl acids (PFAAs), has been linked to activation of peroxisome proliferator-activated receptors (Ppar) in many vertebrates. Here, we present the primary structures, phylogeny, and tissue-specific distributions of the Atlantic cod (*Gadus morhua*) gmPpara1, gmPpara2, gmPparb, and gmPparg, and demonstrate that the carboxylic acids PFHxA, PFOA, PFNA, as well as the sulfonic acid PFHxS, activate gmPpara1 *in vitro,* which was also supported by *in silico* analyses. Intriguingly, a binary mixture of PFOA and the non-activating PFOS produced a higher activation of gmPpara1 compared to PFOA alone, suggesting that PFOS has a potentiating effect on receptor activation. Supporting the experimental data, docking and molecular dynamics simulations of single and double-ligand complexes led to the identification of a putative allosteric binding site, which upon binding of PFOS stabilizes an active conformation of gmPpara1. Notably, binary exposures of gmPpara1, gmPpara2, and gmPparb to model-agonists and PFAAs produced similar potentiating effects. This study provides novel mechanistic insights into how PFAAs may modulate the Ppar signaling pathway by either binding the canonical ligand-binding pocket or by interacting with an allosteric binding site. Thus, individual PFAAs, or mixtures, could potentially modulate the Ppar-signaling pathway in Atlantic cod by interfering with at least one gmPpar subtype.

1. Introduction

Per- and polyfluoroalkyl substances (PFAS) are anthropogenic chemicals that have been used globally in industrial production and consumer products since the late 1940s. PFAS molecules are recognized by their hydrophobic carbon backbone that is either fully or partially saturated with fluorines, and by possessing a hydrophilic functional group. These structures give PFAS both water- and oil-repellant properties that make them useful for consumer and industrial purposes such as surfactants, non-stick coatings, cosmetic additives and flame retardants (Wolf et al., 2008, Kissa, 2001, Renner, 2001, Lau, 2012). The high-energy bonds between the carbons and the fluorines make PFAS highly resistant against abiotic and biotic degradation, and therefore

persistent in nature and biota (Poothong et al., 2012). Long-range transportation, bioaccumulating and biomagnifying properties, as well as observed adverse effects in experimental studies have made PFAS an environmental concern (Conder et al., 2008, Dietz et al., 2008, Houde et al., 2011, Greaves et al., 2012, Gebbink et al., 2016, Boisvert et al., 2019, Routti et al., 2016, Routti et al., 2017, Martin et al., 2004, Kennedy et al., 2004, Lau et al., 2004, Lau et al., 2007, Kelly et al., 2009, Lindstrom et al., 2011, Kwiatkowski et al., 2020). Perfluoroalkyl acids (PFAAs) are a subgroup of PFAS that encompasses perfluoroalkane sulfonic acids (PFSAs) and perfluoroalkyl carboxylic acids (PFCAs), which include the well-recognized perfluorooctanesulfonic acid (PFOS) and perfluorooctanoic acid (PFOA), respectively. In 2009, PFOS was included in the Stockholm Convention on Persistent Organic Pollutants

targeted for elimination of production or strict regulation of its use (Stockholm Convention, 2009). Restrictions on the production and use of PFOA were introduced in 2017 (REACH, 2017), and in 2019 PFOA was enlisted in Annex A in the Stockholm Convention on Persistent Organic Pollutants. However, PFOS and PFOA, in addition to many other PFAS, are still abundant in the environment. This is partly due to their persistence, but also because of the continued release of PFAS-related precursors that are not yet covered by the Stockholm Convention (Moore et al., 2003, Lau et al., 2007).

Research focusing on the molecular mechanisms behind PFAS-mediated toxicity has increased significantly in recent years (Wolf et al., 2008, Bjork et al., 2011, Zhang et al., 2014, Wolf et al., 2014, Beggs et al., 2016, Zhang et al., 2017, Behr et al., 2018, Behr et al., 2020). One mechanism that may cause adverse outcomes from PFAS exposure has been linked to peroxisome proliferator-activated receptor alpha (PPARA) activation in species such as human, rat, mouse, and chicken (Cwinn et al., 2008, Elcombe et al., 2010, Maloney and Waxman, 1999, Rosen et al., 2007, Shipley et al., 2004, Takacs and Abbott, 2007, Vanden Heuvel et al., 2006, Wolf et al., 2008, Behr et al., 2020). PPARs are ligand-activated transcription factors that are members of the nuclear receptor (NR) superfamily. In humans and primates, one of the main functions of PPARs is to regulate the energy homeostasis by controlling the expression of genes involved in the fatty acid utilization and storage (Desvergne and Wahli, 1999, Georgiadi and Kersten, 2012, Colliar et al., 2011, Kliewer et al., 1997). In addition, PPARs are involved in other cellular processes, such as glucose utilization, cell proliferation and differentiation, inflammatory processes, and adipogenesis (Ferré, 2004). The varying functions of PPARs have been linked to the presence of several different subtypes, and their tissue distribution is to a large degree reflected by their different physiological roles (Hihi et al., 2002, Ferré, 2004, Georgiadi and Kersten, 2012, Wagner and Wagner, 2010). Three PPAR paralogs have been described in mammals; PPAR alpha (PPARA), PPAR beta/delta (PPARB/D) (from here on denoted PPARB), and PPAR gamma (PPARG) (Desvergne and Wahli, 1999). The PPAR subtypes share a high degree of sequence similarity (Desvergne and Wahli, 1999), but differ in their tissue distribution, ligand specificity, and target genes in a species-specific manner. Orthologs of the human PPARB and PPARG subtypes have been identified in teleosts, whereas two orthologs of the human PPARA subtype (i. e. Ppara1 and Ppara2) appear to be present in some fish species, such as Atlantic cod (*Gadus morhua*) (Star et al., 2011, Eide et al., 2018), Japanese pufferfish (*Fugu rubripes*) (Maglich et al., 2003), green spotted pufferfish (*Tetraodon nigroviridis*) (Metpally et al., 2007), zebrafish (*Danio rerio*) (Tseng et al., 2011, Bertrand et al., 2007), and turbot (*Scophthalmus maximus*) (Urbatzka et al., 2013).

While Atlantic cod has a high commercial value for North-Atlantic fisheries, it also influences the ecological structure and function of the Arctic ecosystem (Link et al., 2009). Previous studies have detected PFAS in the blood of Baltic cod and in the liver of Atlantic cod along the Norwegian coast (Falandysz et al., 2006, Falandysz et al., 2007, Valdersnes et al., 2017). As a balanced lipid and energy homeostasis is vital for fitness, perturbation of metabolic pathways at critical stages of the life cycle could cause adverse effects. In a recent *in vivo* exposure study with juvenile Atlantic cod and a mixture of PFAS congeners (PFOS, PFNA, PFOA and PFTrDA), proteomics analysis revealed that many enzymes involved in fatty acid β-oxidation pathways were upregulated in the hepatic proteome (Dale et al., 2020). Additionally, lipidomics data indicated an increased hydrolysis of mono-unsaturated triglycerides, followed by hydrolysis into fatty acids channeled towards β-oxidation. These findings suggested that some PFAS congeners might activate Ppara receptors in Atlantic cod. In this study, we present the primary structures, phylogeny, and tissue-specific distribution of the Atlantic cod Ppar proteins (gmPpara1, gmPpara2, gmPparb, and gmPparg). Further, by establishing luciferase-based reporter gene assays, we have assessed the ability of cod Ppar subtypes to bind and become activated by ten PFAAs, including three PFSAs and seven PFCAs. The PFAAs were tested individually, in binary combinations together with a PPAR model-agonist, and as a binary combination of PFOA and PFOS. The experimental analyses were supported by *in silico* structural analyses, including homology modeling, ligand docking, and molecular dynamics simulations. Importantly, this study provides an increased mechanistic insight into how PFAAs can exert its toxic effect through either agonistic Ppar-activation or via interactions with allosteric binding sites present elsewhere in the gmPpar protein structure, and suggest that exposure to an individual PFAA, or mixtures, could modulate the lipid- and carbohydrate metabolism in Atlantic cod, and possibly other teleost fish species.

2. Materials and methods

2.1. Sequence analysis and phylogeny of the gmPpars

The full-length cod Ppar amino acid sequences (gmPpara1, gmPpara2, gmPparb, and gmPparg) were obtained by genome mining in the GadMor3 database (Tørresen et al., 2017). The amino acid sequences were compared to their human orthologs (UniProtKB/ Swiss-Prot: hsPPARA Q07869, hsPPARB(D) Q03181, hsPPARG P37231) through pairwise and multiple sequence alignments (MSA) using the T-Coffee Multiple Sequence Alignment online tool (EMBL-EBI) (Notredame et al., 2000). The alignments were visualized and edited in Jalview v2.11.1.0 (Waterhouse et al., 2009). An MSA was made in T-Coffee (EMBL-EBI) using the cod Ppars and a selected set of PPAR/Ppar sequences obtained from other vertebrate species, including fish, bird, and mammals (protein sequence accession numbers are provided in Supplemental Information Table S1). Based on the MSA, a phylogenetic tree was inferred using a BLOSUM62 model, Bayesian interference (*Coalescent: GMRF Bayesian Skyride*), and Markov Chain Monte Carlo (MCMC) analysis with the BEAST v1.10.4 software package (Drummond and Rambaut, 2007).

2.2. Chemicals

The following compounds were purchased from Sigma-Aldrich, Oslo, Norway, perfluorobutanesulfonic acid (PFBS, $CF_3(CF_2)_3SO_3H$), perfluorohexanesulfonic acid (PFHxS, $CF_3(CF_2)_5SO_3H$), perfluorooctanesulfonic acid (PFOS, $CF_3(CF_2)_7SO_3H$), heptafluorobutyric acid (PFBA, $CF_3(CF_2)_2COOH$), perfluorohexanoic acid (PFHxA, $CF_3(CF_2)_4COOH$), perfluorooctanoic acid (PFOA, $CF_3(CF_2)_6COOH$), perfluorononanoic acid (PFNA, $CF_3(CF_2)_7COOH$), nonadecafluorodecanoic acid (PFDA, $CF_3(CF_2)_8COOH$), perfluoroundecanoic acid (PFUnDA, $CF_3(CF_2)_9COOH$), perfluorotridecanoic acid (PFTrDA, $CF_3(CF_2)_{11}COOH$), WY14643 (PPARA agonist), GW6471 (PPARA antagonist), GW501516 (PPARB agonist), rosiglitazone (PPARG agonist), and tetrabromobisphenol A (TBBPA, brominated flame retardant). Stock solutions were made of each individual compound by dissolving them in dimethyl sulfoxide (DMSO) (>99.9 % pure, Sigma-Aldrich, Oslo, NO).

2.3. Fish and tissue sampling

Atlantic cod were acquired from the Institute of Marine Research (IMR, Bergen, NO) research station at Austevoll (Norway) and from Havbruksstasjonen in Tromsø (Nofima, Norway), and tended to at ILAB (Industrilaboratoriet, Bergen, NO). Cod were kept in 500 L reservoirs with circulating seawater of 8 °C with a 12:12 h (light:dark) photoperiod and fed daily *ad libitum* with commercial feed from EWOS, NO. The cod were sacrificed with a blow to the head in compliance with the Norwegian animal welfare act – regulation on animal experimentation. Cod tissues intended for semi-quantitative qPCR analyses were immediately collected and flash frozen in liquid nitrogen and stored at −80 °C. Heart and brain tissue designated for cloning purposes were immediately used for RNA extraction and isolation.

2.4. Tissue-specific expression of gmppars

Total RNA was extracted from liver, head kidney, gonad, gill, skin, heart, brain, spleen, mid-intestine, stomach, eye, and muscle tissue of juvenile cod specimen (n = 3), using the TRI Reagent® protocol (Sigma-Aldrich, Oslo, NO). cDNA was then synthesized in triplicates from 0.5 µg of extracted RNA using the iScript™ cDNA Synthesis Kit (Bio-Rad, Hercules, CA) according to the manufacturer's protocol. Transcription levels of *gmppara1*, *gmppara2*, *gmpparb*, and *gmpparg* were analyzed with RT-qPCR using LightCycler® 480 SYBR Green I Master (Roche, Basel, CH) and a CFX96 Touch Real-Time PCR Detection System (Bio-Rad, Oslo. NO). The transcript levels of the *gmppars* were normalized across tissues using ubiquitin (*ubi*) and acidic ribosomal protein (*arp*) as reference genes. Mean normalized expression (MNE) of the *gmppars* in the tissues was determined using the geNorm software (Vandesompele et al., 2002) and a normalization factor based on *ubi* and *arp* (M < 0.73). Primer sequences are shown in Supplemental Information Table S2.

2.5. Cloning and sequencing of the gmppars

The *gmppars* were cloned from brain and heart tissue collected from a female cod specimen weighing 466 g (*gmppara1* and *gmpparb* from brain tissue, while *gmppara2* and *gmpparg* from heart tissue). Total RNA was extracted using TRI Reagent® (Sigma-Aldrich, Oslo, NO) according to the manufacturer's instructions. cDNA was synthesized from 2 µg of RNA using SuperScript® III reverse transcriptase (Invitrogen, Carlsbad, CA, USA) together with oligo $(dT)_{12-18}$ and random hexamers according to the manufacturer's protocol. Gene specific primers were designed to amplify the gene fragments encoding the hinge and ligand binding domain (LBD) of the four *gmppar* subtypes. The primers were based on the gene sequences present in the Ensembl cod genome database (*ppara1*: ENSGMOG00000001060, *ppara2*: ENSGMOG00000005934, *pparb*: ENSGMOG00000008225, *pparg*: ENSGMOG00000001375). Detailed information on the cloning and gene-specific primers is presented as supplementary information (Cloning of Atlantic cod Ppar-encoding genes, Table S3, Table S4). The cloned *gmppar* fragments were verified by sequencing according to the BigDye™ Terminator v 3.1 protocol. The Sanger sequencing was performed at the sequencing facility at the Department of Biological Sciences (BIO), University of Bergen, NO, and the nucleotide sequences of the cloned hinge-LBD region of *gmppara1*, *gmppara2*, *gmpparb*, and *gmpparg* have been deposited in Genbank with the accession numbers MW690582, MW690583, MW690584, MW690585, respectively.

2.6. Luciferase reporter gene transactivation assay

Effector plasmids (expressing the cloned gmPpars) were constructed to encode a fusion protein with the GAL4-dependent DNA-binding domain (DBD) and the hinge + ligand-binding domain of the respective gmPpars (i.e., gmPpara1, gmPpara2, gmPparb, and gmPparg). The luciferase reporter gene assays were performed essentially as described previously using COS-7 simian (African green monkey) kidney cells (Lille-Langøy et al. (2015). COS-7 cells were transiently co-transfected with an effector GAL4-gmPpar plasmid, the GAL4-dependent luciferase reporter gene plasmid (mh(1 0 0)x4tk luc), and a β-galactosidase-encoding control plasmid (pCMV-β-Gal) at a mass ratio of 1:10:10 using the TransIT®LT-1 transfection kit (Mirus Bio, Madison, WI, USA) according the manufactures instruction. Subsequently after transfection, the cells were exposed to increasing concentrations of the test ligand (solubilized in 0.5% DMSO) for 24 h. Transactivation of the gmPpar constructs was measured as luciferase enzyme activity using an EnSpire 2300 Multilabel Reader (PerkinElmer, Oslo, NO) and normalized against the enzymatic activity of β-galactosidase as described in Lille-Langøy et al. (2015). GraphPad Prism v.6 was used to produce dose–response curves displaying the average fold activation as normalized luciferase activity relative to control (0.5% DMSO), including standard error of

mean (SEM). One-way ANOVA and Dunnett's multiple comparison test were used to calculate statistically significant fold activation. Expression of the GAL4-gmPpar fusion proteins in the COS7 cells were confirmed with Western Blotting, using mouse anti-Gal4 (DBD) (RK5C1) AC antibodies (Santa Cruz Biotechnology, (cat# sc-510). Mouse anti beta-actin antibodies (ab8224, Abcam) were used for detection of beta-actin as a loading control. A secondary HRP-linked sheep-anti-mouse IgG antibody (NA931V, GE-Healthcare) was used to visualize the primary antibodies. The fluorometric indicator dyes Resazurin (alamarBlue®) and CFDA-AM were used to assess if exposure levels produced any cytotoxic effects (Dayeh et al., 2003). Detailed information on effector plasmid construction and the LRA protocol (LRA protocol, effector plasmid construction, Table S5, Table S6, S LRA protocol) is provided in Supplemental Information. Cytotoxicity data is presented in Fig. S8 and Fig. S9.

2.7. Molecular modeling

2.7.1. Homology modeling

The sequences of gmPpara1 and gmPpara2 were used as input to the I-TASSER server (https://zhanglab.ccmb.med.umich.edu/I-TASSER) to produce homology models, respectively. The best scored homology models were then used in virtual docking calculations with PFOA, PFNA, PFOS, or PFHxS, followed by molecular dynamics simulations. For both the docking calculations and the molecular dynamics simulations, the ligands were taken to be in their ionized forms.

2.7.2. Docking calculations

The AutoDock program version 4.2 was used to dock the PFCAs and PFSAs to the best scored homology models of gmPpara1 and gmPpara2 (Morris et al., 2009). The calculations were piloted using AutoDockTools (ADT) (Morris et al., 2009). The different PFAAs were initially constructed using the Avogadro software (Hanwell et al., 2012). Further details on the docking calculations are provided in Supplemental Information.

2.8. Molecular dynamics simulations

2.8.1. Minimization and molecular dynamics setup

The CHARMM all-atom force field (CHARMM36) was used for describing the protein, ions and the TIP3P model was used for water molecules (MacKerell Jr et al., 1998). The CHARMM Generalized Force Field (CGenFF36) was used for the ligand parameters (Vanommeslaeghe et al., 2010), which were obtained from the ParamChem webserver (available from: https://cgenff.paramchem.org). Further details on the molecular dynamics simulations are provided in Supplemental Information.

2.8.2. Double ligand docking and molecular dynamics simulations

Using the best model structure of gmPpara1 and gmPpara2 docked with PFOA, we performed docking calculations with PFOS. The Autodock4 software was used to place PFOS following the protocol described earlier in this text. The structures having among the best binding energies were extracted and used for subsequent simulations. The parameter and topology files for PFOA and PFOS molecules are those used earlier in this study. These simulations followed the same protocol as described in the previous section for the single-ligand molecular dynamics simulations.

3. Results

3.1. Genome mining and phylogenetic analyses of the Atlantic cod Ppars

Homology searches in the most recent and comprehensive Atlantic cod genome assembly (GadMor3) identified four genes putatively encoding different Ppar subtypes (Table 1). Phylogenetic analyses of the

Table 1
Features and location of PPAR genes in the Atlantic cod genome (GadMor3, and NCBI).

Gene	Accession No.	Chromosome location;	Exons	Nucleotide (bp)	Protein (aa)
gmppara1	XM_030366071	9; Fwd	6	1557	518
gmppara2	XM_030353486	4; Rev	7	1449	482
gmpparb	XM_030352117	1; Fwd	7	1518	505
gmpparg	XM_030374406	13; Rev	8	1632	543

deduced amino acid sequences and PPAR/Ppar protein sequences obtained from a selected set of vertebrate organisms, including fish, bird, and mammalian species, confirmed that the encoded proteins belong to the subfamily 1, group C of nuclear receptors, and that the proteins encoded by the *XM_030366071, XM_030353486, XM_030352117,* and *XM_030374406* transcripts cluster together with other teleost protein sequences within the Ppara1, Ppara2, Pparb, and Pparg sub-branches (Fig. S1). Accordingly, we have named *XM_030366071, XM_030353486, XM_030352117,* and *XM_030374406,* as *gmppara1, gmppara2, gmpparb*, and *gmpparg*, respectively. The *in silico* analyses also revealed the chromosomal location of the four open reading frames as well as the exon/intron distribution of the *gmppar* gene sequences (Table 1).

Sequence alignments of gmPpara1, gmPpara2, gmPparb, and gmPparg with their human orthologs revealed high sequence identities between the PPAR subtypes of these two distantly related species (i.e. 73, 61, 77, and 59 %, respectively) (Fig. 1). As anticipated, the gmPpar proteins share the common structural features found in the nuclear receptor superfamily, including an N-terminal transactivation domain, a DNA-binding domain, a hinge region, and a C-terminal ligand binding domain (LDB) (Fig. 1). Other features are also conserved in the gmPpar aa sequences, including the AF-2 motif important for coregulator interaction in the C-terminal part of the LBD (Andersen et al., 2000, Batista-Pinto et al., 2005), the linker region that allows flexibility between the DBD and LBD upon ligand- and DNA binding (Andersen et al., 2000), as well as helices 1, 3, and 12 (H1, H3, and H12) that form and stabilize the ligand-binding pocket (Fig. 1) (Zheng et al., 2015).

Human PPARs have been extensively studied for therapeutic purposes and the amino acid residues important for binding certain ligands have been identified. Pirinixic acid (WY14643), GW501516, and rosiglitazone are synthetic, selective, and potent agonists of hPPARA, hPPARB, and hPPARG, respectively (Annapurna et al., 2013, Liberato et al., 2012, Nolte et al., 1998, Chandra et al., 2008, Narala et al., 2010, Bernardes et al., 2013, Wu et al., 2017). The WY14643-binding amino acid residues were found positionally conserved in gmPpara1 and gmPpara2, while five out of seven amino acids that bind to GW501516 are conserved in gmPparb (Fig. 1). Notably, only five out of eleven amino acid residues that are recurrently identified as important for binding of rosiglitazone by human PPARG are positionally conserved in gmPparg (Fig. 1). Furthermore, additional stretches of amino acids that are not present in the human orthologs were observed in the transactivation domain of gmPpara1 (49 aa) and gmPparb (65 aa), as well as in the hinge region of gmPpara2 (17 aa) and gmPparg (39 aa) (Fig. 1).

3.2. Tissue-specific expression of gmppars

The tissue specific expressions of the *gmppar* subtypes were assessed with qPCR in twelve different tissues obtained from juvenile Atlantic cod (brain, eye, gill, ovary, head kidney, heart, liver, mid intestine, muscle, skin, spleen, and stomach) (Fig. S2). All four *gmppar* receptors were expressed in each tissue examined. However, the individual expression profiles differed between the receptors, supporting a subtype specific distribution and expression of the *gmppars* in Atlantic cod. Among the twelve tissues, the abundance of *gmppara1* transcripts was highest in liver and heart*,* while *gmppara2* appeared to be ubiquitously expressed

with low transcript abundance in most tissues. *gmpparb* transcripts were most abundant in the ovary, whereas *gmpparg* transcripts were most abundant in the mid intestine and liver.

3.3. In vitro transactivation of the Atlantic cod Ppar subtypes

Effector plasmids encoding the GAL4-gmPpar fusion proteins were transiently transfected into COS-7 cells, and their protein translations were confirmed with protein immunoblotting (Fig. 2 A). The GAL4-gmPpar fusion proteins migrated according to their predicted molecular weights (gmPpara1 = *50.2 kDa,* gmPpara2 = *51.5 kDa,* gmPparb = *50.8 kDa, and* gmPparg = *50.9 kDa)* and were produced in similar amounts. PPAR model-agonists known from mammalian studies were initially used to characterize and confirm ligand-activation of the gmPpar subtypes. WY14643 acted as an agonist for both gmPpara1 and gmPpara2 and produced similar efficacies of 118 and 132 fold activation, respectively (Fig. 2 B). In contrast, the potencies differed between the receptors, where WY14643 was a more potent agonist for gmPpara1 (EC_{50} = 25 μM) compared to gmPpara2 (EC_{50} = 42 μM) (Fig. 2 B). As reported for mammalian PPARB orthologs, GW501516 also activated gmPparb producing an efficacy of 126-fold activation and an EC_{50} corresponding to 2 μM (Fig. 2 C). The GAL4-gmPparg construct however, could not be activated by any of the mammalian PPARG model-agonists tested (e.g., rosiglitazone and TBBPA) and was thus not included in the further analyses (not shown).

3.4. Agonistic activation of gmPpars by PFAAs

A selected set of carboxylated and sulfonated PFAAs of varying carbon backbone length was tested individually for their ability to transactivate the gmPpara1, gmPpara2, and gmPparb subtypes *in vitro*. Three of these carboxylated congeners activated gmPpara1, including PFHxA, PFOA, and PFNA, as well as the sulfonated PFHxS, while neither gmPpara2 nor gmPparb were activated by any of the PFAAs tested (Fig. 3, Fig. S3). The efficacies of the PFCAs were non-linear, demonstrating increased activation with increasing length of the fluorinated carbon backbone, where PFOA exhibited the highest efficacy, and thereafter decreased with PFNA and disappeared with further increased carbon backbone length (Fig. 3).

3.5. Homology modeling of gmPpars and ligand docking of PFAAs

The most notable difference in the primary structure of gmPpara1 and gmPpara2 is the additional stretch of 17 amino acids present in the omega loop region of the gmPPARa2 subtype (Fig. 1). Homology modeling of the gmPpara 3D structures demonstrated that this sequence insertion is positioned between H1 and H3, conceivably resulting in a long loop extension that is situated near both the ligand-binding pocket and the coregulator binding groove (AF-2 motif) (Fig. 4). Ligand-docking analyses of PFOA to the gmPpara structures showed that the carboxyl group of PFOA is oriented toward the C-terminal H12 in gmPpara1 (Fig. 4 A, B). In contrast, PFOA does not find a favorable binding position in gmPpara2. The molecular dynamics (MD) simulations revealed that the omega loop region between H1 and H3 is more flexible in gmPpara2 than gmPpara1 (Fig. 4 E, F). PFOS, which did not activate any of the gmPpara subtypes, is distributed with several different orientations of the sulfur group in the gmPpara1 LBD (Fig. 4 C). Although PFOS appears to find a good orientation in gmPpara2, the MD simulations show significant flexibility in the omega region of both subtypes (Fig. 4 D, G, H). Similar ligand docking analyses and MD simulations with PFHxA, PFNA, and PFHxS, all of which agonistically activated Ppara1, demonstrated favorable orientations of these molecules in the gmPpar1 LBD, as well as less flexibility in the omega region as opposed to gmPpara2 (Fig. S4, S5, S6).

To explore the non-linear effects of PFCA and PFSA congeners as a function of carbon chain length, we carried out docking calculations for
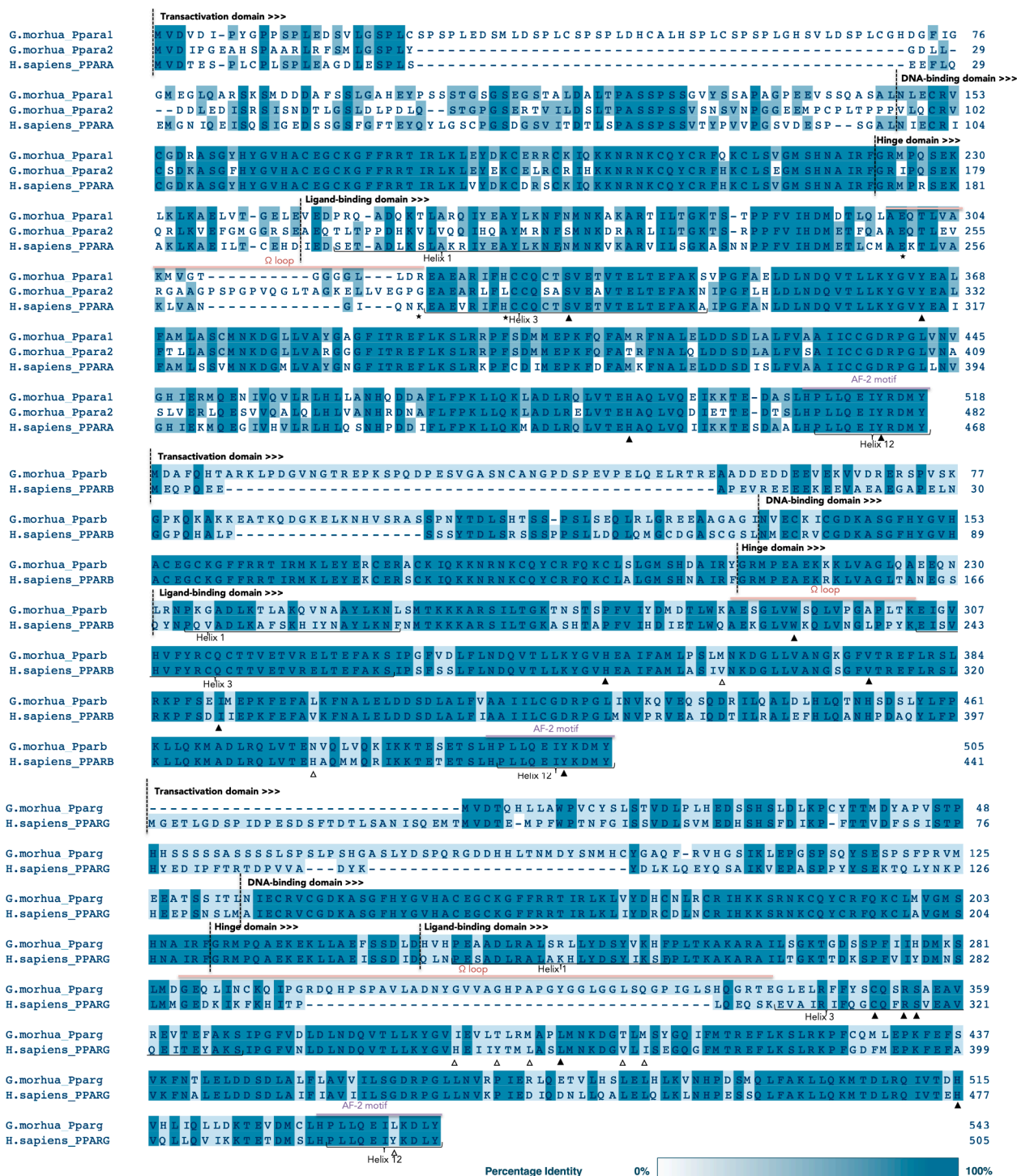
Fig. 1. Multiple sequence alignments of gmPpars and hsPPARs with annotated domains and ligand binding residues. The human PPARs were obtained from Swiss-Prot and used for annotation of the different PPAR domains (indicated by dotted lines and arrows above the alignment), helices (indicated below alignment), flexible loop and AF-2 motif (indicated above alignment). Residues important for ligand binding are indicated as either conserved (▲), or not conserved (△). WY14643 second binding site residues (★). The alignments were edited in Jalview v 2.11.1.0 and have been colored according to percentage identity and conservation.

gmPpara1 with the congeners listed in Table S7. The chain lengths go from (CF2)3 to (CF2)13 for PFCAs, and from (CF2)3 to (CF2)9 for PFSAs. The analysis focused on two observations from the docking calculations, the energy score and the position of the congener in the ligand binding pocket (LBP) and whether the charged group of the ligand interacts with amino acids of H12, a canonical interaction seen in many PPAR/agonist crystal structures. For gmPpara1, this focus was on the interaction with

Tyr514.

We observed a correspondence with the fold induction results shown in Fig. 3, where those compounds that activated gmPpara1 were also compounds that showed a relatively strong binding energy and had a good orientation of the charged head-group (COO– or SO3-) towards Tyr514. Those compounds that did not activate gmPpara1 showed lower binding energies and/or few or no interactions in the LBP. The longer
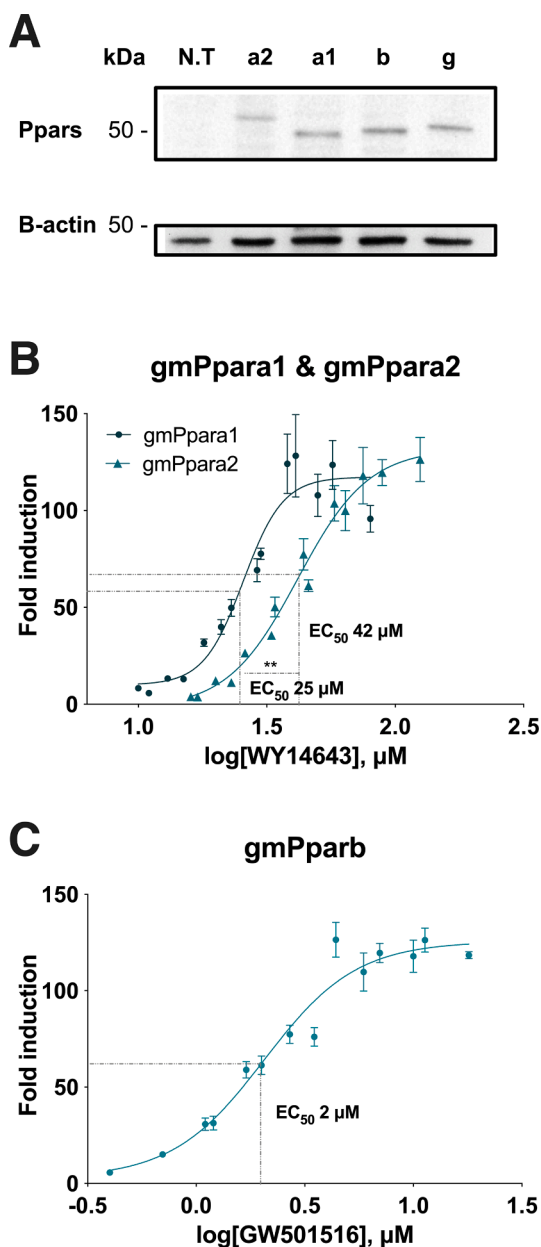
Fig. 2. Synthesis and transactivation of gmPpara1, gmPpara2, gmPparb, and gmPparg in COS-7 cells. A) Protein levels of the GAL4-gmPpar constructs in transfected COS-7 cells were confirmed with Western blotting using mouse-anti Gal4 antibodies. Mouse-anti-beta actin antibodies were used for monitoring protein loading. The secondary HRP-conjugated sheep-anti-mouse IgG antibody was used to visualize the primary antibodies. B & C) Dose-response curves for the activation of Atlantic cod Ppars by WY-14643 (Ppara1 and Ppara2) or GW501516 (Pparb). COS-7 cells were exposed to B) WY14643 (gmPpara1 (0–80 μM) and gmPpara2 (0–125 μM)), or C) GW501516 (gmPparb (0–18 μM)). Each measured point represents mean fold induction of the GAL4-gmPpar constructs relative to the solvent control (DMSO), derived from 12 experimental replicates. Standard error of mean (SEM) is indicated. EC_{50} values are indicated with dotted lines and significant difference between EC_{50} is indicated with ** (<0.005). Non-linear regression analyses were performed in PRISM (GraphPad) to fit a dose–response curve.

chain compounds, such as PFDA, PFUnDA and PFTrDA did not bind in the LBP, nor did the untested compounds, perfluorododecanoic acid (PFDoA, $CF_3(CF_2)_{10}COOH$), perfluorotetradecanoic acid (PFTeA, $CF_3(CF_2)_{12}COOH$) and perfluoropentanoic acid (PFPA, $CF_3(CF_2)_{13}COOH$).

Concerning the active compounds PFHxA, PFOA and PFNA, the docking results show that these compounds all have favorable energy scores and they display interactions with Tyr514. PFOA has a significantly higher number of conformations satisfying our criteria of energy score and placement in the binding pocket (25% of the docked conformations). PFOA is also the compound showing the highest activity. Concerning the compound perfluoroheptanoic acid (PFHpA, $CF_3(CF_2)_5COOH$) the docking results show that it has a relatively favorable binding energy and orientation. The shorter chain compounds, even though they docked with relatively good interaction energies with Tyr514, are likely to be too short to fill the LBP and stabilize the complex. Similar conclusions were reached in Ren et al. (2016). The observation that orientation of the compound towards the Tyr514 and the interaction energy are correlated with activity was also made for the PFSA congeners.

3.6. Binary exposures reveal potentiating effects of PFAAs on gmPpar activation

Potential antagonistic properties of the PFAA congeners were also assessed with the luciferase reporter gene assay. Initially, gmPpara1, gmPpara2, and gmPparb were activated with fixed concentration of model agonists (equal to their EC_{20}) and exposed to increasing concentrations of GW6471 or GSK3787, which are known to antagonize human PPARA and PPARB, respectively. As expected, a decrease in the activation of the receptors was observed, and the IC_{50} values of gmPpara1, gmPpara2, and gmPparb were determined to 0.4 μM, 3.0 μM, and 0.8 μM, respectively (Fig. S7). Corresponding experiments were also performed where gmPpara1 was activated with fixed concentrations of either PFHxS or PFOA, representing a sulfonated and carboxylated PFAA agonist. Also here, a decrease in gmPpara1 activity with increasing GW6471 concentrations were observed, supporting that WY14643, as well as the sulfonated and carboxylated PFAA congeners, bind to the canonical ligand-binding pocket and compete with GW6471 for this binding site (Fig. S7).

Binary exposures were further carried out with individual PFAA compounds together with a fixed concentration of WY14643 (gmPpara1, gmPpara2) or GW501516 (gmPparb). However, no antagonistic effects were observed with any of the PFAAs on either of the Ppar subtypes. Intriguingly, we observed on the contrary that the majority of the PFAAs that did not demonstrate any agonistic features produced a dose-dependent potentiation of the receptor activation of gmPpara1, gmPpara2, and gmPparb (Fig. 5). The strongest potentiating effect was observed with gmPparb, where PFDA increased the GW501516-mediated activity close to seven fold (Fig. 5). The increased efficacies of gmPpara1, gmPpara2, and gmPparb induced by co-exposure to PFAAs may suggest the presence of a second binding site available for PFAA molecules in these receptors.

To assess if interaction effects also could occur with exposures to mixtures of PFAAs, gmPpara1 was exposed to a binary combination of PFOA and PFOS (Fig. 6 A, B, C). As observed previously (Fig. 3), PFOS alone was not able to activate gmPpara1, while PFOA demonstrated a dose-dependent activation of the receptor (Fig. 6 A). However, exposure to equimolar mixtures of PFOA and PFOS elicited an increased activation of gmPpara1 compared to PFOA exposure alone (Fig. 6 A), supporting that PFOS potentiates the PFOA-mediated activation. The same exposure regimes did not activate gmPpara2 (Fig. 6 B). As an alternative approach to study interaction effects, gmPpara1 was coexposed to PFOA (increasing concentrations) together with fixed concentrations of PFOS (either 50 or 100 μM). Notably, the addition of fixed PFOS concentrations produced a higher fold induction in the PFOA-mediated dose–response curve at the lower to mid-range concentrations of PFOA (Fig. 6 C). Since none of the dose–response curves reached a plateau of activation, EC50 values could not be calculated. However, a left-shift in the dose–response curves was observed as the background concentration of PFOS increased (Fig. 6 C).
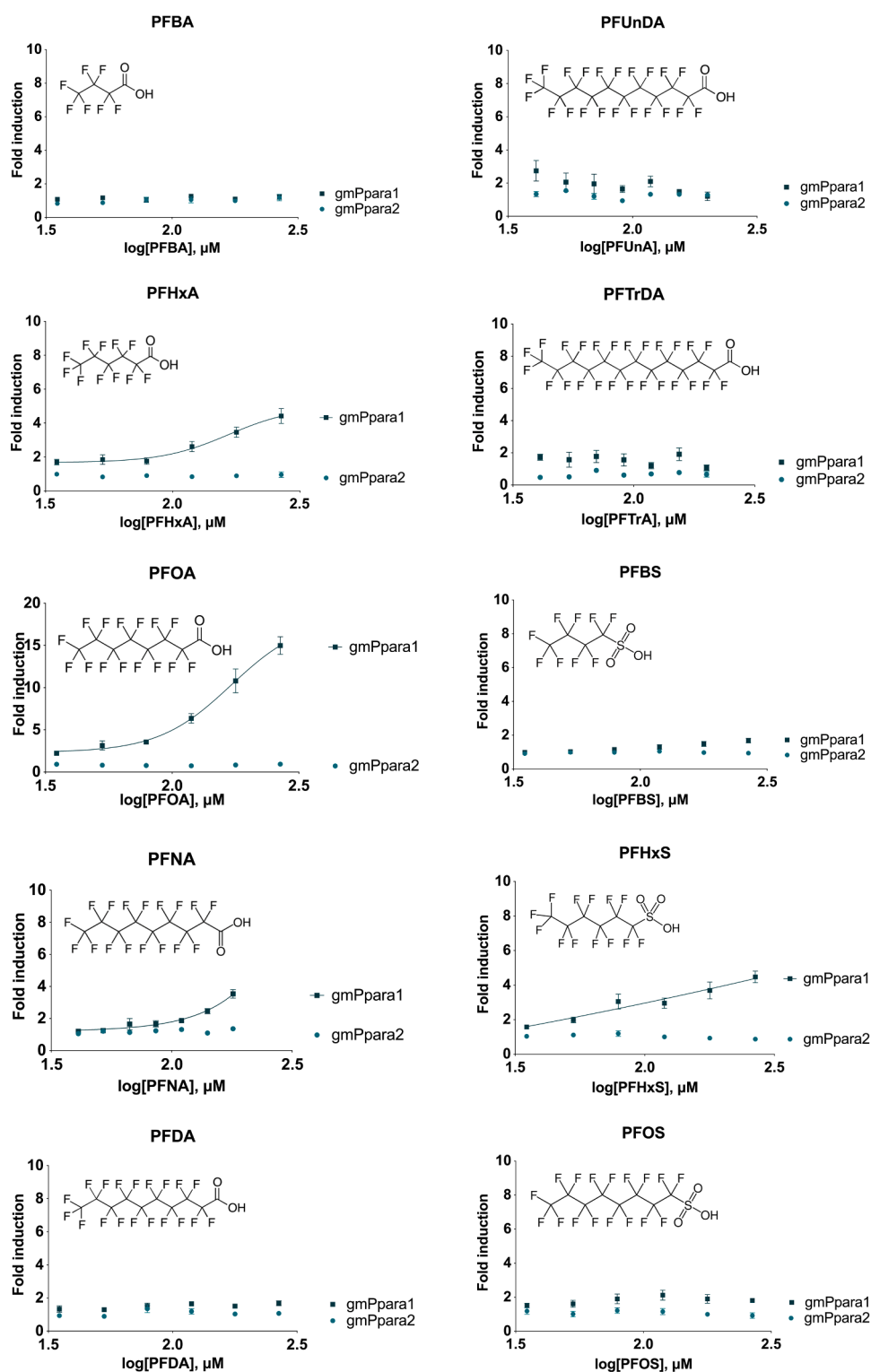
Fig. 3. Ligand activation of the gmPpara1 and gmPpara2 constructs exposed to single PFAAs. Dose-response curves showing average fold induction ± standard error of the mean (SEM) (GraphPad, Prism). A consistent trend of > 2-fold induction was set as a minimum requirement before considering the dose–response as consistent. Exposure concentrations of PFCAs were as follows: PFBA, PFHxA, PFOA, PFDA (35–267 µM), PFNA (41–180 µM), PFUnDA, PFTrDA (41–200 µM). Exposure concentrations to PFSAs were as follows: PFBS, PFHxS, PFOS (35–267 µM). All data points are based on three experimental replicates, and the LRAs were repeated three times (except for PFUnDA and PFTrDA, which are based on three technical replicates).

3.7. Double-ligand modeling

To further investigate the potentiating effect of PFOS, molecular dynamics simulations were done for complexes where PFOS was docked to gmPpara1 and gmPpara2 already docked with PFOA. Molecular dynamics simulations were carried out for favorable two-ligand complexes following the same protocol as that for the single ligand simulations. The docking analysis revealed a family of structures where both PFOA and PFOS were favorably situated in or near the ligand-binding pocket and the omega loop. Subsequent molecular dynamics (MD) simulations of the gmPpara1 complex revealed that the PFOS molecule reorients itself in such a way as to occupy an alternative binding site where the hydrophobic fluorocarbon chain places itself in a hydrophobic pocket formed by the beta sheets, H2 and H3. Analysis of the molecular dynamics simulations shows that the PFOS in this alternative binding pocket leads to further stabilization of the omega loop region between
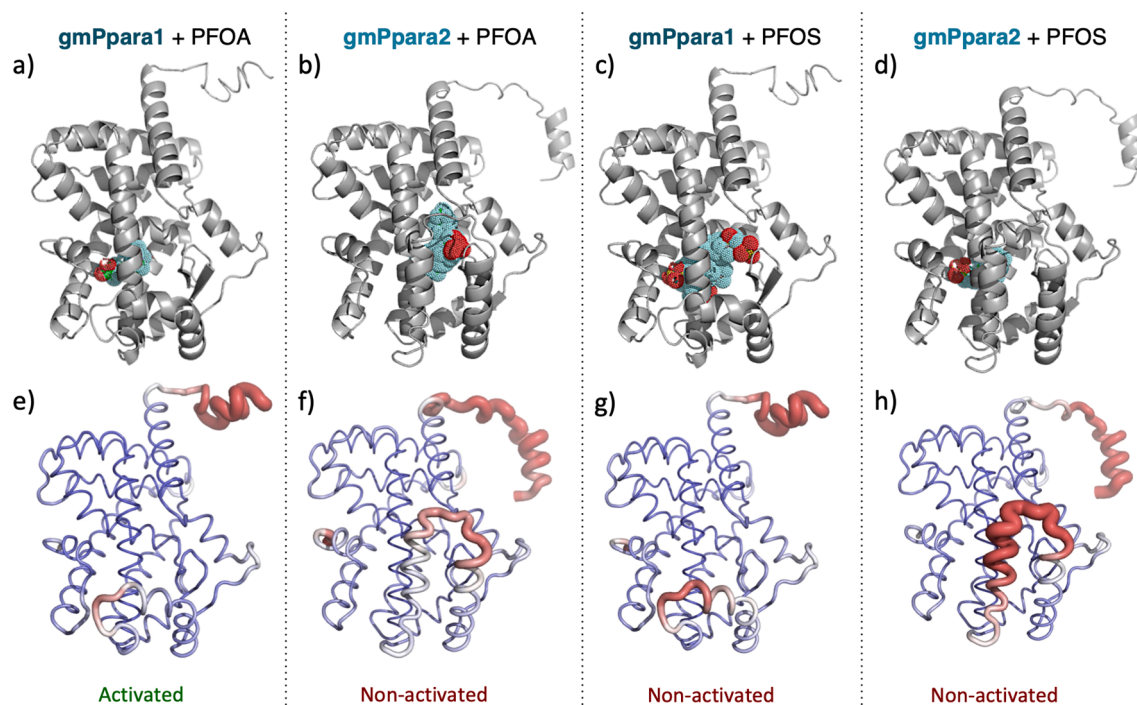
Fig. 4. Results from ligand docking analyses and molecular dynamic simulations of gmPpara1 and gmPpara2; representative best-scoring complexes from docking, a) gmPpara1 with PFOA, b) gmPpara2 with PFOA, c) gmPpara1with PFOS and d) gmPpara2 with PFOS. The RMS fluctuations are represented by a putty drawing. The thicker, intensely red colored tube, the greater the flexibility. e) gmPpara1 with PFOA, f) gmPpara2 with PFOA, g) gmPpara1with PFOS and h) gmPpara2 with PFOS. The activation response to the ligand is indicated below the structures. (For interpretation of the references to colour in this figure legend, the reader is referred to the web version of this article.)

H1 and H3 with respect to gmPpara1 in complex with PFOA alone (Fig. 7 A, B), leading to a structurally more stable ligand binding domain and in particular the region near the coactivator binding site. No such stabilization was observed in the simulations of the gmPpara2 dual ligand complex (Fig. 7 C, D).

4. Discussion

Genome mining combined with phylogenetic analyses identified the genes encoding the gmPpara1, gmPpara2, gmPparb, and gmPparg proteins in the Atlantic cod genome. Tissue-specific expression analyses revealed that all *gmppar* subtypes were ubiquitously expressed and similar abundances of their transcripts were found in brain, eye, gill, head kidney, muscle, skin, and spleen. Elevated transcript levels of *gmppara1* were observed in liver and heart, while *gmppara2* was expressed in all tissues at lower levels. The expression of *ppara1* and *ppara2* reported from turbot (*Scophthalmus maximus*) demonstrated the opposite pattern (Urbatzka et al. (2013), but the *gmppara1* expression is more in line with tissue expression of *ppara1* reported from sea bream (*Sparus aurata*), plaice (*Pleuronectes platessa*), and brown trout (*Salmo trutta*), (although these teleosts only have one Ppara subtype) (Batista-Pinto et al., 2005, Leaver et al., 2005), as well as the expression pattern of the mammalian PPARA that also predominate in tissues with high metabolic rates, such as liver and heart (Escher et al., 2001, Ferré, 2004, Bookout et al., 2006, Georgiadi and Kersten, 2012). The abundant occurrence of a PPAR/Ppar subtype in a certain tissue may reflect its physiological function. Mammalian PPARA is mainly, but not exclusively, involved in releasing stored energy through peroxisomal and mitochondrial fatty acid catabolism (Hihi et al., 2002). Atlantic cod uses the liver as a lipid depot for energy storage (Karlsen et al., 2006, Kjær et al., 2009), and the high abundance of *gmppara1* in liver may support a role of this receptor in regulating the release of stored energy. The exact function of the second Ppara subtype in teleosts is still not well understood, but *gmppara2* may be more active at certain developmental

stages, or in a tissue type that was not examined in this study. Although less studied, mammalian PPARB tissue expression appears to be ubiquitous (Georgiadi and Kersten, 2012, Ferré, 2004), and it is believed to be involved in balancing energy homeostasis and muscular development (Wagner and Wagner, 2010). This could also be the case for *gmpparb* as it was expressed in all tissues examined, although elevated levels were observed in the ovary where it was most abundant of all subtypes. Similarly, Batista-Pinto et al. (2005) also found the expression of *pparb* in brown trout to be high in the reproductive organ, among other tissues. Mammalian PPARB has been linked to a role in embryo implantation (Hihi et al., 2002), so it is possible that the gmPparb has a reproductive role, e.g. in involvement in ovarian tissue remodelling or ovary maturation. Mammalian PPARG is expressed in adipose tissue and lower intestine, where its main role is believed to be promotion of energy storage by lipid accumulation and adipogenesis (Hihi et al., 2002, Ferré, 2004). The higher expression of *gmpparg* in the liver and mid intestine is in agreement with these tissues being important for absorbing lipids and storing them as excess energy in accordance with Atlantic cod physiology. High mRNA levels of *pparg* in the intestine has also been found in other teleost species (Luo et al., 2015, Leaver et al., 2005, You et al., 2017).

Transactivation studies were carried out with the GAL4/UAS system and the LBDs from the different Ppar subtypes. This assay does not include the inherent DNA binding domain of the receptor, nor receptor-specific response elements controlling the reporter, which potentially may affect activation profiles. However, the GAL4/UAS system is commonly used to study activation of a great variety of nuclear receptors and allows for comparative studies of both receptor subtypes and receptors obtained from different species. The mammalian PPAR agonists, WY14643 and GW501516, were in this assay potent agonists for gmPpara1/gmPpara2 (EC_{50} 25 μM/EC_{50} 42 μM) and gmPparb (EC_{50} 2 μM), respectively, and produced similar EC_{50} values as reported from other teleost species (e.g., GW501516 EC_{50} approx. 1 μM) (Leaver et al., 2005, Kondo et al., 2007, Colliar et al., 2011, Leaver et al., 2007). In
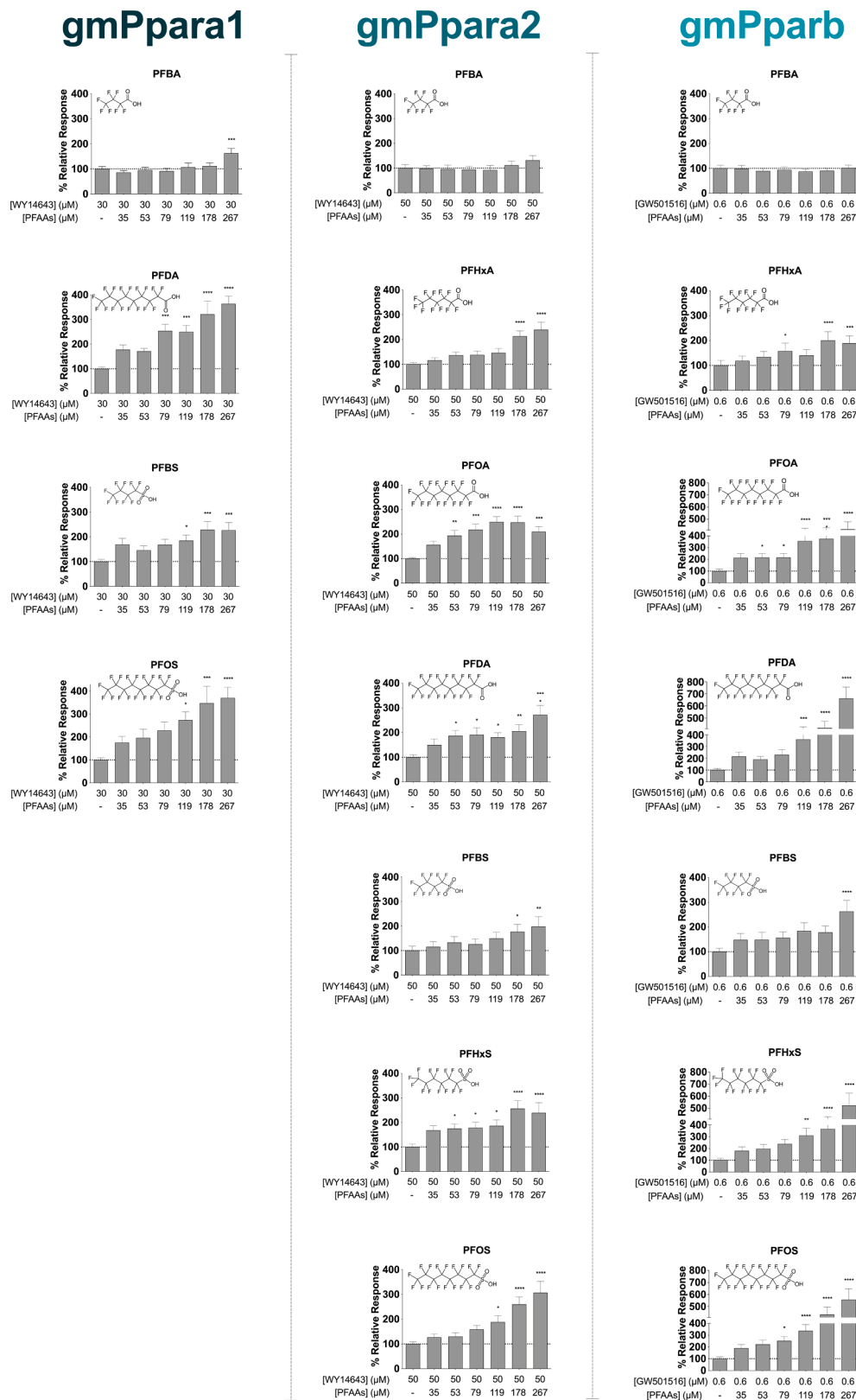
Fig. 5. gmPpara1, gmPpara2, and gmPparb exposed to a binary combination of fixed concentrations ofmodel-agonist and increasing concentrations of seven different PFAAs. All data points are based on three experimental replicates, and the LRAs were repeated at least 3 times. Significant % Relative Response compared to control is indicated with * <0.05, ** <0.005, *** < 0.0005, **** < 0.0001 (GraphPad, Prism).
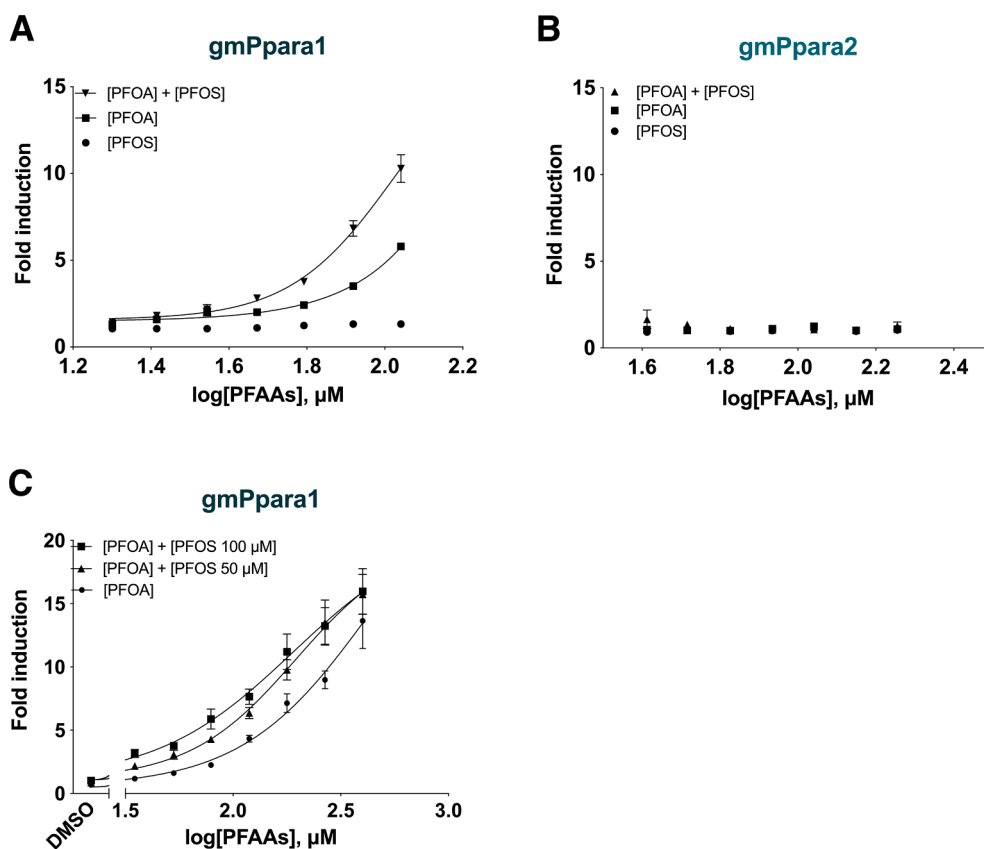
Fig. 6. Ligand activation of gmPpara1 and gmPpara2 constructs exposed to binary mixtures of PFOA and PFOS. Dose-response-relationship showing average fold induction ± standard error of the mean (SEM) (GraphPad, Prism). A) gmPpara1 exposed to PFOA and PFOS individually, and in a binary equimolar mixture (20–110 µM), B) gmPpara2 exposed to PFOA and PFOS individually, and in a binary equimolar mixture (41–180 µM). C) gmPpara1 exposed to PFOA, and in binary combinations together with fixed concentrations of PFOS. Exposures were conducted with PFOA in increasing concentration (35–267 µM), while PFOS is kept at fixed concentrations of either 50 or 1 0 0 µM. All data points are based on three experimental replicates and the LRAs were repeated three times.

contrast, the typical mammalian PPARG model-agonist, rosiglitazone, in addition to other PPARG ligands tested (e.g. TBBPA) was not able to activate the gmPparg subtype, although protein immunoblotting confirmed that the GAL4-gmPparg fusion protein was synthesized in transfected COS-7 cells. Notably, only five out of eleven amino acid positions important for binding rosiglitazone in human PPARG are conserved in the gmPparg protein sequence, which most likely contribute to the lack of activation. In line with the findings in this study, the absence of teleost Pparg-stimulated target gene expression or ligand activation by rosiglitazone and fatty acids have been reported in several other studies on plaice, sea bream, medaka (*Oryias latipes*), and Japanese pufferfish (Kondo et al., 2007, Kondo et al., 2010, Colliar et al., 2011, He et al., 2012). As mentioned, gmPparg had 39 additional amino acids in the region spanning the omega loop, which has also been reported for other teleost species (Batista-Pinto et al., 2005, You et al., 2017, Boukouvala et al., 2004, Raingeard et al., 2009, Andersen et al., 2000, Wafer et al., 2017, Cho et al., 2009, Zheng et al., 2015, He et al., 2015, Kondo et al., 2007, Leaver et al., 2005). Both He et al. (2015) and Zheng et al. (2015) suggested from *in silico* analyses that these additional amino acids in the omega loop region would cause teleost Pparg to fold into a different tertiary structure compared to the human ortholog, and possibly rendering it unable to become activated by fatty acids and synthetic ligands normally activating human PPARG.

The PPARA subtype is recurrently shown to be a target of PFAAs exposure in both mammalian and teleost species (Leaver et al. (2005), (Cwinn et al., 2008, Elcombe et al., 2010, Maloney and Waxman, 1999, Rosen et al., 2007, Shipley et al., 2004, Takacs and Abbott, 2007, Vanden Heuvel et al., 2006, Wolf et al., 2008, Behr et al., 2020, Dale et al., 2020). Accordingly, we show that gmPpara1 is activated by PFAAs, specifically by three PFCAs (i.e. PFHxA, PFOA and PFNA), but only one PFSA (PFHxS). Our results emphasize that the functional group in PFAS molecules has an important role in agonistic recognition and receptor activation. However, several studies have shown that other

sulfonates (e.g., PFOS) can act as mammalian PPARA agonists in transactivation assays, although being less potent compared to the carboxylated congeners (Shipley et al., 2004, Heuvel et al., 2006, Takacs and Abbott, 2007, Wolf et al., 2008). Furthermore, the length of the PFCAs carbon backbone appears as determinative for gmPpara1 activation efficacy, which increased with the length of the fluorinated carbon backbone up to C7 (PFOA), and thereafter decreased with further increasement in carbon backbone length. The docking results suggested that both the interaction with Tyr514 of H12, as well as the chain lengths contribute to these non-linear effects. Short-chain compounds, even though they may bind in the LBP and interact with Tyr514, are likely to be too short to stabilize the LBD, in particular the omega loop, while the mid-length compounds, which show activity, can both bind in the LBP and stabilize the LBD as demonstrated by the molecular dynamics simulations for those compounds. Activity then decreases with chain length as the chains become too long to bind the LBP. These results are in agreement with what has been demonstrated previously in mammalian GAL4-PPARA ligand activation assays, which also reported a correlation between the length of the carbon backbone and receptor activation (Wolf et al., 2008, Buhrke et al., 2013, Behr et al., 2020). However, the correlations observed for activation of gmPpara1 with both PFAA carbon-chain length and functional group show some discrepancies from that observed for mouse and human PPARA, which also differ between them (Takacs and Abbott, 2007). CASTp topology calculations (Tian et al., 2018) on experimental and homology model PPAR alpha structures suggest that the PPARA/Ppara ligand binding pockets from the different species vary in volume (not shown), which may be implicated in these differential efficacies.

Short-chain PFAAs have been shown to have a higher elimination rate and a lower bioaccumulation potential and are currently being evaluated for replacing the commercial use of PFOA and PFOS (Bowman, 2015). It is therefore interesting to notice that the short-chain PFAAs, i.e. PFBA and PFBS, did not demonstrate any agonistic potential
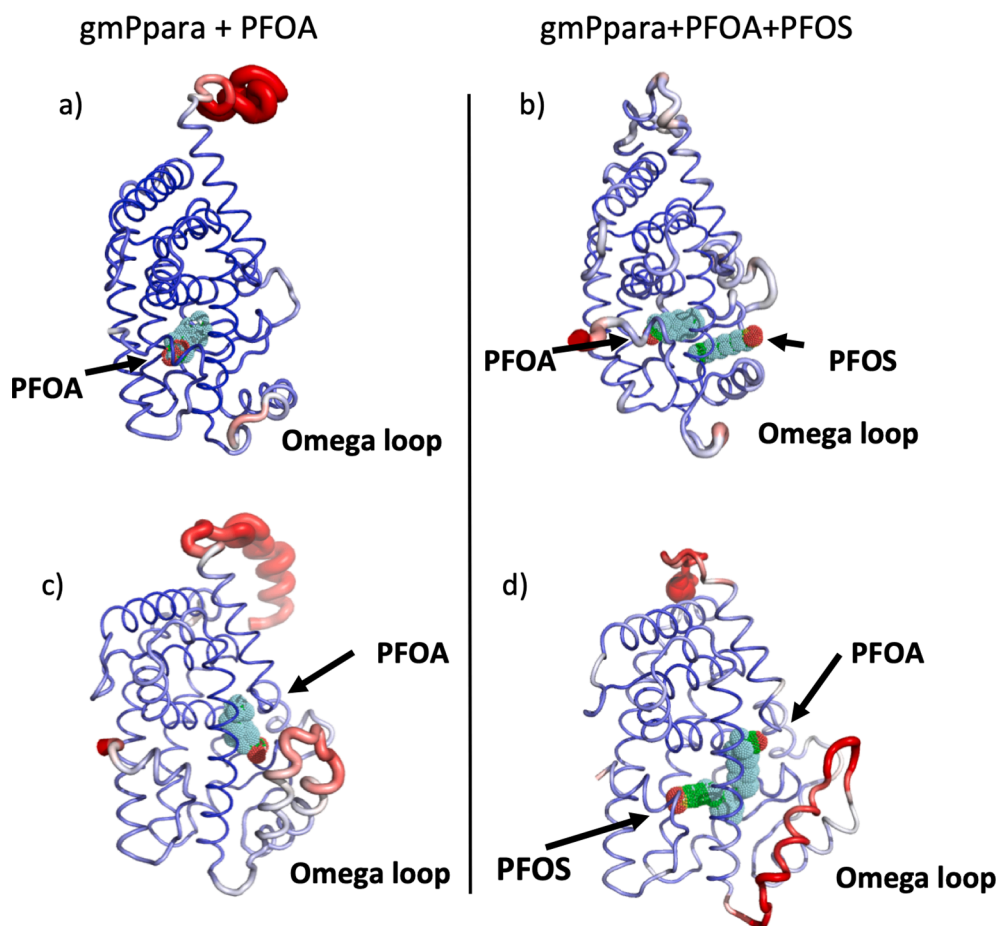
gmPpara + PFOA

a)

PFOA

Omega loop

gmPpara+PFOA+PFOS

b)

PFOA ← → PFOS

Omega loop

c)

← PFOA

Omega loop

d)

← PFOA

PFOS →

Omega loop

Fig. 7. Results from the double ligand docking analyses and molecular dynamics simulations of gmPpara1 and gmPpara2. The RMS fluctuations are represented by a putty drawing. The thicker, more intensely red colored tube, the greater the flexibility. a) gmPpara1 with PFOA, b) gmPpara1 with PFOA and PFOS, c) gmPpara2 with PFOA, and d) gmPpara2 with PFOA and PFOS. (For interpretation of the references to colour in this figure legend, the reader is referred to the web version of this article.)

to gmPpar1a. This is in agreement with other studies showing that short-chain PFAS have relatively low activity and weaker binding affinity towards nuclear receptors in comparison to long-chain PFAS (Goodrum et al., 2021). It has thus been assumed that shorter-chain PFAS are less toxic, although more and more studies are questioning this assumption. Nevertheless, it must be emphasized that short-chain PFAAs are as persistent in nature as long-chain PFAAs and more knowledge regarding other possible adverse effects of the new generation of PFAS molecules on wildlife and humans are still of great demand.

Similar to Ppargs in teleosts, it has been reported that also Ppara in several teleost species contain additional amino acids in their omega loop region in comparison to the human ortholog (You et al., 2017, Boukouvala et al., 2004, Raingeard et al., 2009, Kondo et al., 2007). In gmPpara2, the additional stretch of 17 amino acids in the omega loop may explain the observed discrepancies between gmPpara1 and gmPpara2 regarding both PFAAs activation, as well as the differences in activation profiles produced by WY14643. This was supported by homology modeling of the gmPpara 3D structure, which confirmed that the longer loop extension in gmPpara2 is situated between H1 and H3 near the ligand-binding pocket, as well as in close proximity to the coregulator binding site. The ligand-docking analyses of PFOA to the gmPpara1 and gmPpara2 3D models further indicated that the carboxyl group of PFOA was positioned in a favorable orientation in the ligand-binding pocket for stabilizing the LBD and promoting an active conformation of the gmPpara1. A similar orientation was also observed in the crystal structure of human PPARG complexed with decanoic acid and the PGC-1a coactivator peptide (Malapaka et al., 2012). Ligand docking analyses also produced favorable orientations of the other PFAAs that activated gmPpara1 (i.e. PFHxA, PFNA, and PFHxS), demonstrating a good agreement between the observed experimental

ligand-activation results *in vitro* and those obtained *in silico*. In contrast, the docking results showed that PFOA does not find an energetically favorable position in gmPpara2. Potential consequences of this result were highlighted by molecular dynamics (MD) simulations demonstrating that the loop region between H1 and H3, which is the region where the additional amino acids are situated in gmPpara2, is more flexible in gmPpara2 than in gmPpara1 and may therefore interfere with ligand and/or co-activator binding. Despite failing to activate either of the cod Ppara subtypes, the docking calculations positioned PFOS in a more favorable orientation in the gmPpara2 ligand-binding pocket, while its orientation was more varied in gmPpara1. However, the MD simulations of these complexes indicated high flexibility in the H1-H3 region of gmPpara1 and gmPpara2, which suggests structural instability in both LBDs and a possible explanation for the inability of PFOS to activate either gmPpara1 or gmPpara2. Notably, a similar difference in binding of PFOA and PFOS has been observed with another nuclear receptor. Beggs et al. (2016) reported that *in silico* docking of these two compounds to HNF4 alpha, an orphan receptor believed to bind fatty acids, showed that PFOA orients into a similar conformation as the endogenous ligand, while PFOS bound to a different binding site and had a different conformation compared to either the endogenous ligand or PFOA.

Binary exposures with a PFAA together with either the WY14643 or GW501516 model-agonists caused an unprecedented potentiation (increase) of the gmPpara1/gmPpara2 and gmPparb receptor activities, which may suggest the existence of a second binding site for PFAA molecules. Moreover, a binary exposure of Ppara1 with PFOA and PFOS revealed that PFOS potentiated the PFOA-mediated Ppara1 activation, demonstrating that this interaction effect also can occur in the presence of a PFAA agonist. Notably, it has previously been demonstrated that

two WY14643 molecules can bind simultaneously to two different sites in a crystal structure of human PPARA (Bernardes et al. (2013). One of the WY14643 molecules binds conventionally in the ligand-binding pocket and stabilizes the positioning of H12 in the active receptor conformation, while the second molecule binds to an alternative site sandwiched between the flexible omega loop and H3, and its carboxyl end is in contact with the residues E251, K266, and H274 (marked with ★, Fig. 1). Mutagenesis of the non-canonical binding site combined with functional analyses suggested that human PPARA becomes activated in a bipartite manner where binding of the second WY14643 molecule further stabilizes helix 12 in a fashion that promotes the interaction with coactivator proteins (Bernardes et al., 2013). Two of these amino acids in the second binding site for WY14643 in human PPAR are conserved in gmPpara1, apart from the conservative substitution of K266R. On the other hand, this site appears to be disrupted in gmPpara2 where two of these residues are substituted with amino acids possessing other chemical properties, i.e. K266G and H274L.

In human PPARA, the aromatic rings of WY14643 makes hydrophobic contacts with I241, L254, I272, C275, V332, among others in the second binding site. These amino acids are conserved in both gmPpara1 (I289, L302, I323, C326, V383) and gmPpara2 (I240 L253, I287, C290, V347), and equivalent residues in human PPARG are I249, I262, I281, C285 and I341, respectively. These human PPARG amino acids constitute an alternative binding site previously identified by Hughes et al. (2014a) using NMR analysis. In the average structure calculated from the end of the simulation of gmPpara1 complexed with PFOA and PFOS, the PFOS molecule makes contacts with I289, I323, C326 Val383 in the alternative binding site. Such interactions could provide an explanation for the mechanism of the potentiating effect of PFOS on the PFOA-mediated activation of the gmPpara1 subtype observed in the luciferase reporter gene assay. Different scenarios of "hyperactivation" through allosteric coupling of the human PPARG by a second ligand have also been suggested by e.g. 1) binding of two molecules of the same ligand, one to the canonical binding site and stabilizing LBD, and the second ligand to an alternative site, or 2) binding of a second ligand when the canonical LBD was already occupied and stabilized by an endogenous ligand (Hughes et al., 2014b). For the nuclear receptor PXR, it has been demonstrated that mixtures of xenobiotics that individually exhibited low efficacies could act together to synergistically activate this receptor. Crystallographic studies revealed that PXR can accommodate multiple binding modes, including those where two different xenobiotics are bound simultaneously in the ligand binding pocket (Delfosse et al., 2021). Although our experimental data and *in silico* analyses support a scenario where a PFAA molecule binds to a putative second binding site in the gmPpar protein structures, the binding site for PFAAs is perhaps not the same as the second binding site for WY14643 in human PPARA and may also not be common for the different Atlantic cod Ppar subtypes. However, the molecular dynamics simulations suggest that PFOS could bind in an alternative binding site that exploits similar interactions as WY14643 in human PPARA.

A recent *in vivo* study demonstrated that exposure to a PFAA-mixture consisting of PFOS, PFOA, PFNA and PFTrDA, at environmentally relevant concentrations affected the Ppar signaling pathways in Atlantic cod liver (Dale et al., 2020). Here, we provide supporting data by demonstrating that PFOA and PFNA can act as agonists and activate gmPpara1 *in vitro*. In addition, we have demonstrated that simultaneous exposure to PFOA and PFOS potentiates the activity of gmPpara1, where PFOS significantly enhanced the receptor activation compared to the activation observed with PFOA alone. Wolf et al. (2014) also reported interaction effects in a binary mixture of PFOA and PFOS when exposing human PPARA, although the predicted effect was additive in the lower concentration range (1–32 μM), the effect exceeded the predicted additive response at higher concentrations. In contrast to gmPpara1, the co-exposure of PFOA and PFOS did not activate gmPpara2, thereby inferring that the presence of a ligand that is able to bind and stabilize the LBD is essential to allow for a second ligand to modulate Ppara2

activity via another interaction site. The double-ligand docking, and molecular dynamics simulations provided support to this theory, as the double-ligand complex (gmPpara2 + PFOA + PFOS) did not show any additional structural stability in the flexible omega loop with respect to the single ligand complex gmPpara2 + PFOA. The results presented in this study suggest that a PFAA, seemingly unable to activate Ppara, may potentiate the toxicity when co-occurring in conjunction with a receptor-activating PFAA congener. This finding also emphasizes one of the major shortcomings in performing only single compound risk assessment.

In summary, the hinge region and LBD from gmPpara1, gmPpara2, gmPparb, and gmPparg were cloned and further subjected to functional characterization of ligand activation using Gal4/UAS-based luciferase reporter gene assays. PFHxA, PFOA, PFNA, as well as PFHxS, activated solely the gmPpara1 subtype. In accordance with other studies, we could observe a relationship between receptor activation and carbon backbone length, as well as the functional group of the PFAAs. Intriguingly, a potentiating effect was observed when exposing the gmPpara1/a2 and gmPparb to a binary combination of one PFAA and the corresponding model-agonist, as well as when co-exposing gmPpara1 to PFOA and PFOS. This suggests that PFAS molecules that on their own are unable to act as Ppar agonists may still modulate receptor activities when present together with an agonist. PFAAs are continuously released into the environment as they are still being used for commercial purposes. The compiling indications of gmPpars having a second binding site in their LBDs make PFAAs (singly or in mixtures) possible modulators of gmPpar signaling pathways, but acting in an unprecedented fashion. PFAAs disrupting the lipid- and energy metabolism through Ppar activation in Atlantic cod could potentially lead to adverse effects affecting physiological parameters such as growth, reproduction, and survival, a finding that is potentially transferrable to other teleost species.

CRediT authorship contribution statement

Sofie Søderstrøm: Formal analysis, Investigation, Writing – original draft, Visualization. **Roger Lille-Langøy:** Investigation, Writing – review & editing. **Fekadu Yadetie:** Investigation, Writing – review & editing. **Mateusz Rauch:** Investigation. **Ana Milinski:** Investigation. **Annick Dejaegere:** Writing – review & editing, Resources. **Roland H. Stote:** Formal analysis, Investigation, Writing – original draft, Visualization, Resources. **Anders Goksøyr:** Writing – review & editing, Conceptualization, Funding acquisition. **Odd André Karlsen:** Writing – original draft, Conceptualization, Funding acquisition, Project administration, Supervision, Formal analysis.

Declaration of Competing Interest

The authors declare that they have no known competing financial interests or personal relationships that could have appeared to influence the work reported in this paper.

Acknowledgements

Intensif) for computing resources.

Appendix A. Supplementary material

Supplementary data to this article can be found online at https://doi.org/10.1016/j.envint.2022.107203.

References

Andersen, Ø., Eijsink, V.G.H., Thomassen, M., 2000. Multiple variants of the peroxisome proliferator-activated receptor (PPAR) γ are expressed in the liver of Atlantic salmon (Salmo salar). Gene 255 (2), 411–418.

Annapurna, H.V., Apoorva, B., Ravichandran, N., Arun, K.P., Brindha, P., Swaminathan, S., Vijayalakshmi, M., Nagarajan, A., 2013. Isolation and in silico evaluation of antidiabetic molecules of Cynodon dactylon (L.). Journal of Molecular Graphics and Modelling 39, 87–97.

BATISTA-PINTO, C., RODRIGUES, P., ROCHA, E. & LOBO-DA-CUNHA, A. 2005. Identification and organ expression of peroxisome proliferator activated receptors in brown trout (Salmo trutta f. fario). *Biochimica et Biophysica Acta (BBA)-Gene Structure and Expression,* 1731, 88-94.

Beggs, K.M., McGreal, S.R., McCarthy, A., Gunewardena, S., Lampe, J.N., Lau, C., Apte, U., 2016. The role of hepatocyte nuclear factor 4-alpha in perfluorooctanoic acid-and perfluorooctanesulfonic acid-induced hepatocellular dysfunction. Toxicology and applied pharmacology 304, 18–29.

Behr, A.-C., Lichtenstein, D., Braeuning, A., Lampen, A., Buhrke, T., 2018. Perfluoroalkylated substances (PFAS) affect neither estrogen and androgen receptor activity nor steroidogenesis in human cells in vitro. Toxicology letters 291, 51–60.

Behr, A.-C., Plinsch, C., Braeuning, A., Buhrke, T., 2020. Activation of human nuclear receptors by perfluoroalkylated substances (PFAS). Toxicology in Vitro 62, 104700.

Bernardes, A., Souza, P.C., Muniz, J.R., Ricci, C.G., Ayers, S.D., Parekh, N.M., Godoy, A. S., Trivella, D.B., Reinach, P., Webb, P., 2013. Molecular mechanism of peroxisome proliferator-activated receptor α activation by WY14643: a new mode of ligand recognition and receptor stabilization. Journal of molecular biology 425, 2878–2893.

Bertrand, S., Thisse, B., Tavares, R., Sachs, L., Chaumot, A., Bardet, P.-L., Escrivà, H., Duffraisse, M., Marchand, O., Safi, R., 2007. Unexpected novel relational links uncovered by extensive developmental profiling of nuclear receptor expression. PLoS genetics 3, e188.

Bjork, J., Butenhoff, J., Wallace, K.B., 2011. Multiplicity of nuclear receptor activation by PFOA and PFOS in primary human and rodent hepatocytes. Toxicology 288, 8–17.

Boisvert, G., Sonne, C., Rigét, F.F., Dietz, R., Letcher, R.J., 2019. Bioaccumulation and biomagnification of perfluoroalkyl acids and precursors in East Greenland polar bears and their ringed seal prey. Environmental pollution 252, 1335–1343.

Bookout, A.L., Jeong, Y., Downes, M., Ruth, T.Y., Evans, R.M., Mangelsdorf, D.J., 2006. Anatomical profiling of nuclear receptor expression reveals a hierarchical transcriptional network. Cell 126, 789–799.

Boukouvala, E., Antonopoulou, E., Favre-Krey, L., Diez, A., Bautista, J.M., Leaver, M.J., Tocher, D.R., Krey, G., 2004. Molecular characterization of three peroxisome proliferator-activated receptors from the sea bass (Dicentrarchus labrax). Lipids 39, 1085–1092.

Bowman, J. S. 2015. Fluorotechnology is critical to modern life: the FluoroCouncil counterpoint to the Madrid Statement. *Environmental health perspectives,* 123, A112-A113.

Buhrke, T., Kibellus, A., Lampen, A., 2013. In vitro toxicological characterization of perfluorinated carboxylic acids with different carbon chain lengths. Toxicology letters 218, 97–104.

Chandra, V., Huang, P., Hamuro, Y., Raghuram, S., Wang, Y., Burris, T.P., Rastinejad, F., 2008. Structure of the intact PPAR-γ–RXR-α nuclear receptor complex on DNA. Nature 456, 350–356.

Cho, H.K., Kong, H.J., Nam, B.-H., Kim, W.-J., Noh, J.-K., Lee, J.-H., Kim, Y.-O., Cheong, J., 2009. Molecular cloning and characterization of olive flounder (Paralichthys olivaceus) peroxisome proliferator-activated receptor γ. General and comparative endocrinology 163, 251–258.

Colliar, L., Sturm, A., Leaver, M.J., 2011. Tributyltin is a potent inhibitor of piscine peroxisome proliferator-activated receptor α and β. Comparative Biochemistry and Physiology Part C: Toxicology & Pharmacology 153, 168–173.

Conder, J.M., Hoke, R.A., Wolf, W.D., Russell, M.H., Buck, R.C., 2008. Are PFCAs bioaccumulative? A critical review and comparison with regulatory criteria and persistent lipophilic compounds. Environmental science & technology 42, 995–1003.

Convention, S. 2009. Stockholm Convention Online available at:. http://chm.pops.int/Implementation/IndustrialPOPs/PFOS/Overview/tabid/5221/Default.aspx (2009).

Cwinn, M.A., Jones, S.P., Kennedy, S.W., 2008. Exposure to perfluorooctane sulfonate or fenofibrate causes PPAR-α dependent transcriptional responses in chicken embryo hepatocytes. Comparative Biochemistry and Physiology Part C: Toxicology & Pharmacology 148, 165–171.

Dale, K., Yadetie, F., Müller, M.B., Pampanin, D.M., Gilabert, A., Zhang, X., Tairova, Z., Haarr, A., Lille-Langøy, R., Lyche, J.L., 2020. Proteomics and lipidomics analyses reveal modulation of lipid metabolism by perfluoroalkyl substances in liver of Atlantic cod (Gadus morhua). Aquatic Toxicology 105590.

Dayeh, V.R., Bols, N.C., Schirmer, K., Lee, L.E., 2003. The use of fish-derived cell lines for investigation of environmental contaminants. *Curr Protoc Toxicol,* Chapter 1, 1–17.

Delfosse, V., Huet, T., Harrus, D., Granell, M., Bourguet, M., Gardia-Parège, C., Chiavarina, B., Grimaldi, M., le Mével, S., Blanc, P., 2021. Mechanistic insights into the synergistic activation of the RXR–PXR heterodimer by endocrine disruptor mixtures. In: Proceedings of the National Academy of Sciences, p. 118.

Desvergne, B., Wahli, W., 1999. Peroxisome proliferator-activated receptors: nuclear control of metabolism 1. Endocrine reviews 20, 649–688.

Dietz, R., Bossi, R., Riget, F.F., Sonne, C., Born, E., 2008. Increasing perfluoroalkyl contaminants in east Greenland polar bears (Ursus maritimus): a new toxic threat to the Arctic bears. Environmental science & technology 42, 2701–2707.

Drummond, A.J., Rambaut, A., 2007. BEAST: Bayesian evolutionary analysis by sampling trees. BMC evolutionary biology 7, 1–8.

Eide, M., Rydbeck, H., Tørresen, O.K., Lille-Langøy, R., Puntervoll, P., Goldstone, J.V., Jakobsen, K.S., Stegeman, J., Goksøyr, A., Karlsen, O.A., 2018. Independent losses of a xenobiotic receptor across teleost evolution. Scientific reports 8, 10404.

Elcombe, C.R., Elcombe, B.M., Foster, J.R., Farrar, D.G., Jung, R., Chang, S.-C., Kennedy, G.L., Butenhoff, J.L., 2010. Hepatocellular hypertrophy and cell proliferation in Sprague-Dawley rats following dietary exposure to ammonium perfluorooctanoate occurs through increased activation of the xenosensor nuclear receptors PPARα and CAR/PXR. Archives of toxicology 84 (10), 787–798.

Escher, P., Braissant, O., Basu-Modak, S., Michalik, L., Wahli, W., Desvergne, B., 2001. Rat PPARs: quantitative analysis in adult rat tissues and regulation in fasting and refeeding. Endocrinology 142 (10), 4195–4202.

Falandysz, J., Taniyasu, S., Gulkowska, A., Yamashita, N., Schulte-Oehlmann, U., 2006. Is fish a major source of fluorinated surfactants and repellents in humans living on the Baltic Coast? Environmental science & technology 40, 748–751.

Falandysz, J., Taniyasu, S., Yamashita, N., Rostkowski, P., Zalewski, K., Kannan, K., 2007. Perfluorinated compounds in some terrestrial and aquatic wildlife species from Poland. Journal of Environmental Science and Health Part A 42, 715–719.

FERRÉ, P. 2004. The biology of peroxisome proliferator-activated receptors. *Diabetes,* 53, S43-S50.

Gebbink, W.A., Bossi, R., Rigét, F.F., Rosing-Asvid, A., Sonne, C., Dietz, R., 2016. Observation of emerging per-and polyfluoroalkyl substances (PFASs) in Greenland marine mammals. Chemosphere 144, 2384–2391.

Georgiadi, A., Kersten, S., 2012. Mechanisms of gene regulation by fatty acids. Advances in Nutrition: An International Review Journal 3, 127–134.

Goodrum, P.E., Anderson, J.K., Luz, A.L., Ansell, G.K., 2021. Application of a framework for grouping and mixtures toxicity assessment of PFAS: A closer examination of dose-additivity approaches. Toxicological Sciences 179, 262–278.

Greaves, A.K., Letcher, R.J., Sonne, C., Dietz, R., Born, E.W., 2012. Tissue-specific concentrations and patterns of perfluoroalkyl carboxylates and sulfonates in East Greenland polar bears. Environmental science & technology 46, 11575–11583.

Hanwell, M.D., Curtis, D.E., Lonie, D.C., Vandermeersch, T., Zurek, E., Hutchison, G.R., 2012. Avogadro: an advanced semantic chemical editor, visualization, and analysis platform. Journal of cheminformatics 4, 1–17.

He, A.-Y., Liu, C.-Z., Chen, L.-Q., Ning, L.-J., Qin, J.-G., Li, J.-M., Zhang, M.-L., Du, Z.-Y., 2015. Molecular characterization, transcriptional activity and nutritional regulation of peroxisome proliferator activated receptor gamma in Nile tilapia (Oreochromis niloticus). General and comparative endocrinology 223, 139–147.

He, S., Liang, X.-F., Qu, C.-M., Huang, W., Shen, D., Zhang, W.-B., Mai, K.-S., 2012. Identification, organ expression and ligand-dependent expression levels of peroxisome proliferator activated receptors in grass carp (Ctenopharyngodon idella). Comparative Biochemistry and Physiology Part C: Toxicology & Pharmacology 155, 381–388.

Heuvel, J.P.V., Thompson, J.T., Frame, S.R., Gillies, P.J., 2006. Differential activation of nuclear receptors by perfluorinated fatty acid analogs and natural fatty acids: a comparison of human, mouse, and rat peroxisome proliferator-activated receptor-α,-β, and-γ, liver X receptor-β, and retinoid X receptor-α. Toxicological Sciences 92, 476–489.

Hihi, A., Michalik, L., Wahli, W., 2002. PPARs: transcriptional effectors of fatty acids and their derivatives. Cellular and Molecular Life Sciences 59, 790–798.

Houde, M., de Silva, A.O., Muir, D.C., Letcher, R.J., 2011. Monitoring of perfluorinated compounds in aquatic biota: an updated review: PFCs in aquatic biota. Environmental science & technology 45, 7962–7973.

Hughes, T.S., Giri, P.K., de Vera, I.M.S., Marciano, D.P., Kuruvilla, D.S., Shin, Y., Blayo, A.-L., Kamenecka, T.M., Burris, T.P., Griffin, P.R., Kojetin, D.J., 2014a. An alternate binding site for PPARγ ligands Nat. Commun. 5 (1).

Hughes, T.S., Giri, P.K., de Vera, I.M.S., Marciano, D.P., Kuruvilla, D.S., Shin, Y., Blayo, A.-L., Kamenecka, T.M., Burris, T.P., Griffin, P.R., 2014b. An alternate binding site for PPARγ ligands. Nature communications 5, 1–13.

Karlsen, Ø., Norberg, B., Kjesbu, O., Taranger, G., 2006. Effects of photoperiod and exercise on growth, liver size, and age at puberty in farmed Atlantic cod (Gadus morhua L.). ICES Journal of Marine Science 63, 355–364.

Kelly, B.C., Ikonomou, M.G., Blair, J.D., Surridge, B., Hoover, D., Grace, R., Gobas, F.A., 2009. Perfluoroalkyl contaminants in an Arctic marine food web: trophic magnification and wildlife exposure. Environmental science & technology 43, 4037–4043.

Kennedy, G.L., Butenhoff, J.L., Olsen, G.W., O'Connor, J.C., Seacat, A.M., Perkins, R.G., Biegel, L.B., Murphy, S.R., Farrar, D.G., 2004. The toxicology of perfluorooctanoate. Critical reviews in toxicology 34, 351–384.

Kissa, E., 2001. Fluorinated surfactants and repellents. CRC Press.

Kjær, M.A., Vegusdal, A., Berge, G.M., Galloway, T.F., Hillestad, M., Krogdahl, Å., Holm, H., Ruyter, B., 2009. Characterisation of lipid transport in Atlantic cod (Gadus morhua) when fasted and fed high or low fat diets. Aquaculture 288, 325–336.

Kliewer, S.A., Sundseth, S.S., Jones, S.A., Brown, P.J., Wisely, G.B., Koble, C.S., Devchand, P., Wahli, W., Willson, T.M., Lenhard, J.M., 1997. Fatty acids and eicosanoids regulate gene expression through direct interactions with peroxisome

proliferator-activated receptors α and γ. Proceedings of the National Academy of Sciences 94, 4318–4323.

Kondo, H., Misaki, R., Gelman, L., Watabe, S., 2007. Ligand-dependent transcriptional activities of four torafugu pufferfish Takifugu rubripes peroxisome proliferator-activated receptors. General and comparative endocrinology 154, 120–127.

Kondo, H., Misaki, R., Watabe, S., 2010. Transcriptional activities of medaka Oryzias latipes peroxisome proliferator-activated receptors and their gene expression profiles at different temperatures. Fisheries Science 76, 167.

Kwiatkowski, C.F., Andrews, D.Q., Birnbaum, L.S., Bruton, T.A., Dewitt, J.C., Knappe, D. R., Maffini, M.V., Miller, M.F., Pelch, K.E., Reade, A., 2020. Scientific Basis for Managing PFAS as a Chemical Class. Environmental Science & Technology Letters 7, 532–543.

Lau, C., 2012. Perfluoroalkyl acids: recent research highlights. Reproductive Toxicology 33 (4), 405–409.

Lau, C., Anitole, K., Hodes, C., Lai, D., Pfahles-Hutchens, A., Seed, J., 2007. Perfluoroalkyl acids: a review of monitoring and toxicological findings. Toxicological sciences 99, 366–394.

Lau, C., Butenhoff, J.L., Rogers, J.M., 2004. The developmental toxicity of perfluoroalkyl acids and their derivatives. Toxicology and applied pharmacology 198, 231–241.

Leaver, M.J., Boukouvala, E., Antonopoulou, E., Diez, A., Favre-Krey, L., Ezaz, M.T., Bautista, J.M., Tocher, D.R., Krey, G., 2005. Three peroxisome proliferator-activated receptor isotypes from each of two species of marine fish. Endocrinology 146, 3150–3162.

Leaver, M.J., Ezaz, M.T., Fontagne, S., Tocher, D.R., Boukouvala, E., Krey, G., 2007. Multiple peroxisome proliferator-activated receptor β subtypes from Atlantic salmon (Salmo salar). Journal of Molecular Endocrinology 38, 391–400.

Liberato, M.V., Nascimento, A.S., Ayers, S.D., Lin, J.Z., Cvoro, A., Silveira, R.L., Martínez, L., Souza, P.C., Saidemberg, D., Deng, T., 2012. Medium chain fatty acids are selective peroxisome proliferator activated receptor (PPAR) γ activators and pan-PPAR partial agonists. PLoS One 7, e36297.

Lille-Langøy, R., Goldstone, J.V., Rusten, M., Milnes, M.R., Male, R., Stegeman, J.J., Blumberg, B., Goksøyr, A., 2015. Environmental contaminants activate human and polar bear (Ursus maritimus) pregnane X receptors (PXR, NR1I2) differently. Toxicology and applied pharmacology 284, 54–64.

Lindstrom, A.B., Strynar, M.J., Libelo, E.L., 2011. Polyfluorinated compounds: past, present, and future. ACS 45 (19), 7954–7961.

Link, J.S., Bogstad, B., Sparholt, H., Lilly, G.R., 2009. Trophic role of Atlantic cod in the ecosystem. Fish and Fisheries 10, 58–87.

Luo, S., Huang, Y., Xie, F., Huang, X., Liu, Y., Wang, W., Qin, Q., 2015. Molecular cloning, characterization and expression analysis of PPAR gamma in the orange-spotted grouper (Epinephelus coioides) after the Vibrio alginolyticus challenge. Fish & shellfish immunology 43 (2), 310–324.

Mackerell JR, A. D., Bashford, D., Bellott, M., Dunbrack JR, R. L., Evanseck, J. D., Field, M. J., Fischer, S., Gao, J., Guo, H. & Ha, S. 1998. All-atom empirical potential for molecular modeling and dynamics studies of proteins. The journal of physical chemistry B, 102, 3586-3616.

Maglich, J.M., Caravella, J.A., Lambert, M.H., Willson, T.M., Moore, J.T., Ramamurthy, L., 2003. The first completed genome sequence from a teleost fish (Fugu rubripes) adds significant diversity to the nuclear receptor superfamily. Nucleic acids research 31, 4051–4058.

Malapaka, R.R., Khoo, S., Zhang, J., Choi, J.H., Zhou, X.E., Xu, Y., Gong, Y., Li, J., Yong, E.-L., Chalmers, M.J., 2012. Identification and mechanism of 10-carbon fatty acid as modulating ligand of peroxisome proliferator-activated receptors. Journal of Biological Chemistry 287, 183–195.

Maloney, E.K., Waxman, D.J., 1999. trans-Activation of PPARα and PPARγ by structurally diverse environmental chemicals. Toxicology and applied pharmacology 161, 209–218.

Martin, J.W., Smithwick, M.M., Braune, B.M., Hoekstra, P.F., Muir, D.C., Mabury, S.A., 2004. Identification of long-chain perfluorinated acids in biota from the Canadian Arctic. Environmental Science & Technology 38, 373–380.

Metpally, R.P.R., Vigneshwar, R., Sowdhamini, R., 2007. Genome inventory and analysis of nuclear hormone receptors in Tetraodon nigroviridis. Journal of biosciences 32, 43–50.

Moore, J., Rodericks, J., Turnbull, D. & Warren-Hicks, W. 2003. Environmental and Health Assessment of Perfluorooctane Sulfonic Acid and its Salts. St. Paul, MN M, 3.

Morris, G.M., Huey, R., Lindstrom, W., Sanner, M.F., Belew, R.K., Goodsell, D.S., Olson, A.J., 2009. AutoDock4 and AutoDockTools4: Automated docking with selective receptor flexibility. Journal of computational chemistry 30, 2785–2791.

Narala, V.R., Adapala, R.K., Suresh, M.V., Brock, T.G., Peters-Golden, M., Reddy, R.C., 2010. Leukotriene B4 is a physiologically relevant endogenous peroxisome proliferator-activated receptor-α agonist. Journal of Biological Chemistry 285, 22067–22074.

Nolte, R.T., Wisely, G.B., Westin, S., Cobb, J.E., 1998. Ligand binding and co-activator assembly of the peroxisome proliferator-activated receptor-gamma. Nature 395, 137.

Notredame, C., Higgins, D.G., Heringa, J., 2000. T-Coffee: A novel method for fast and accurate multiple sequence alignment. Journal of molecular biology 302, 205–217.

Poothong, S., Boontanon, S.K., Boontanon, N., 2012. Determination of perfluorooctane sulfonate and perfluorooctanoic acid in food packaging using liquid chromatography coupled with tandem mass spectrometry. Journal of hazardous materials 205, 139–143.

Raingeard, D., Bilbao, E., Sáez-Morquecho, C., de Cerio, O.D., Orbea, A., Cancio, I., Cajaraville, M.P., 2009. Cloning and transcription of nuclear receptors and other toxicologically relevant genes, and exposure biomarkers in European hake (Merluccius merluccius) after the Prestige oil spill. Marine genomics 2 (3-4), 201–213.

REACH 2017. REACH Commission Regulation (EU) 2017/1000 of 13 June 2017 Amending Annex XVII to Regulation (EC) no 1907/2006 of the European Parliament and of the Council Concerning the Registration, Evaluation, Authorisation and Restriction of Chemicals (REACH) as Regards Perfluorooctanoic Acid (PFOA), Its Salts and PFOA-related Substances Online available at http://eur-lex.europa.eu/eli/reg/2017/1000/oj.

Ren, X.-M., Qin, W.-P., Cao, L.-Y., Zhang, J., Yang, Y., Wan, B., Guo, L.-H., 2016. Binding interactions of perfluoroalkyl substances with thyroid hormone transport proteins and potential toxicological implications. Toxicology 366, 32–42.

Renner, R., 2001. Growing concern over perfluorinated chemicals. ACS Publications. 35 (7), 154A–160A.

Rosen, M.B., Thibodeaux, J.R., Wood, C.R., Zehr, R.D., Schmid, J.E., Lau, C., 2007. Gene expression profiling in the lung and liver of PFOA-exposed mouse fetuses. Toxicology 239, 15–33.

Routti, H., Aars, J., Fuglei, E., Hanssen, L., Lone, K., Polder, A., Pedersen, Å.Ø., Tartu, S., Welker, J.M., Yoccoz, N.G., 2017. Emission changes dwarf the influence of feeding habits on temporal trends of per-and polyfluoroalkyl substances in two Arctic top predators. Environmental Science & Technology 51, 11996–12006.

Routti, H., Gabrielsen, G.W., Herzke, D., Kovacs, K.M., Lydersen, C., 2016. Spatial and temporal trends in perfluoroalkyl substances (PFASs) in ringed seals (Pusa hispida) from Svalbard. Environmental Pollution 214, 230–238.

Shipley, J.M., Hurst, C.H., Tanaka, S.S., Deroos, F.L., Butenhoff, J.L., Seacat, A.M., Waxman, D.J., 2004. Trans-activation of PPARα and induction of PPARα target genes by perfluorooctane-based chemicals. Toxicological sciences 80, 151–160.

Star, B., Nederbragt, A.J., Jentoft, S., Grimholt, U., Malmstrøm, M., Gregers, T.F., Rounge, T.B., Paulsen, J., Solbakken, M.H., Sharma, A., 2011. The genome sequence of Atlantic cod reveals a unique immune system. Nature 477, 207–210.

Takacs, M.L., Abbott, B.D., 2007. Activation of mouse and human peroxisome proliferator–activated receptors (α, β/δ, γ) by perfluorooctanoic acid and perfluorooctane sulfonate. Toxicological Sciences 95, 108–117.

Tian, W., Chen, C., Lei, X., Zhao, J., Liang, J., 2018. CASTp 3.0: computed atlas of surface topography of proteins. Nucleic acids research 46, W363–W367.

Tørresen, O.K., Star, B., Jentoft, S., Reinar, W.B., Grove, H., Miller, J.R., Walenz, B.P., Knight, J., Ekholm, J.M., Peluso, P., 2017. An improved genome assembly uncovers prolific tandem repeats in Atlantic cod. BMC genomics 18, 95.

Tseng, Y.-C., Chen, R.-D., Lucassen, M., Schmidt, M.M., Dringen, R., Abele, D., Hwang, P.-P., 2011. Exploring uncoupling proteins and antioxidant mechanisms under acute cold exposure in brains of fish. PLoS One 6, e18180.

Urbatzka, R., Galante-Oliveira, S., Rocha, E., Castro, L., Cunha, I., 2013. Tissue expression of PPAR-alpha isoforms in Scophthalmus maximus and transcriptional response of target genes in the heart after exposure to WY-14643. Fish physiology and biochemistry 39, 1043–1055.

Valdersnes, S., Nilsen, B.M., Breivik, J.F., Borge, A., Maage, A., 2017. Geographical trends of PFAS in cod livers along the Norwegian coast. PloS one 12, e0177947.

Vanden Heuvel, J. P., Thompson, J. T., Frame, S. R. & Gillies, P. J. 2006. Differential activation of nuclear receptors by perfluorinated fatty acid analogs and natural fatty acids: a comparison of human, mouse, and rat peroxisome proliferator-activated receptor-α,-β, and-γ, liver X receptor-β, and retinoid X receptor-α. Toxicological Sciences, 92, 476-489.

Vandesompele, J., de Preter, K., Pattyn, F., Poppe, B., van Roy, N., de Paepe, A., Speleman, F., 2002. Accurate normalization of real-time quantitative RT-PCR data by geometric averaging of multiple internal control genes. Genome biology 3 (research0034), 1.

Vanommeslaeghe, K., Hatcher, E., Acharya, C., Kundu, S., Zhong, S., Shim, J., Darian, E., Guvench, O., Lopes, P., Vorobyov, I., 2010. CHARMM general force field: A force field for drug-like molecules compatible with the CHARMM all-atom additive biological force fields. Journal of computational chemistry 31, 671–690.

Wafer, R., Tandon, P. & Minchin, J. E. 2017. The Role of Peroxisome Proliferator-Activated Receptor Gamma (PPARG) in Adipogenesis: Applying Knowledge from the Fish Aquaculture Industry to Biomedical Research. Frontiers in endocrinology, 8.

Wagner, K.-D., Wagner, N., 2010. Peroxisome proliferator-activated receptor beta/delta (PPARβ/δ) acts as regulator of metabolism linked to multiple cellular functions. Pharmacology & therapeutics 125, 423–435.

Waterhouse, A.M., Procter, J.B., Martin, D.M., Clamp, M., Barton, G.J., 2009. Jalview Version 2—a multiple sequence alignment editor and analysis workbench. Bioinformatics 25, 1189–1191.

Wolf, C.J., Rider, C.V., Lau, C., Abbott, B.D., 2014. Evaluating the additivity of perfluoroalkyl acids in binary combinations on peroxisome proliferator-activated receptor-α activation. Toxicology 316, 43–54.

Wolf, C.J., Takacs, M.L., Schmid, J.E., Lau, C., Abbott, B.D., 2008. Activation of mouse and human peroxisome proliferator– activated receptor alpha by perfluoroalkyl acids of different functional groups and chain lengths. Toxicological Sciences 106, 162–171.

Wu, C.-C., Baiga, T.J., Downes, M., la Clair, J.J., Atkins, A.R., Richard, S.B., Fan, W., Stockley-Noel, T.A., Bowman, M.E., Noel, J.P., 2017. Structural basis for specific ligation of the peroxisome proliferator-activated receptor δ. Proceedings of the National Academy of Sciences 114, E2563–E2570.

You, C., Jiang, D., Zhang, Q., Xie, D., Wang, S., Dong, Y., Li, Y., 2017. Cloning and expression characterization of peroxisome proliferator-activated receptors (PPARs) with their agonists, dietary lipids, and ambient salinity in rabbitfish Siganus canaliculatus. Comparative Biochemistry and Physiology Part B: Biochemistry and Molecular Biology 206, 54–64.

Zhang, L., Ren, X.-M., Wan, B., Guo, L.-H., 2014. Structure-dependent binding and activation of perfluorinated compounds on human peroxisome proliferator-activated receptor γ. Toxicology and applied pharmacology 279, 275–283.

Zhang, Y.-M., Dong, X.-Y., Fan, L.-J., Zhang, Z.-L., Wang, Q., Jiang, N., Yang, X.-S., 2017. Poly-and perfluorinated compounds activate human pregnane X receptor. Toxicology 380, 23–29.

Zheng, J.-L., Zhuo, M.-Q., Luo, Z., Pan, Y.-X., Song, Y.-F., Huang, C., Zhu, Q.-L., Hu, W., Chen, Q.-L., 2015. Peroxisome proliferator-activated receptor gamma (PPARγ) in yellow catfish Pelteobagrus fulvidraco: molecular characterization, mRNA expression and transcriptional regulation by insulin in vivo and in vitro. General and comparative endocrinology 212, 51–62.